

Concepts in the design and engineering of single-molecule electronic devices

Na Xin¹, Jianxin Guan¹, Chenguang Zhou¹, Xinjiani Chen¹, Chunhui Gu¹, Yu Li¹, Mark A. Ratner², Abraham Nitzan³, J. Fraser Stoddart^{1,2*} and Xuefeng Guo^{1*}

Abstract | Over the past two decades, various techniques for fabricating nano-gapped electrodes have emerged, promoting rapid development in the field of single-molecule electronics, on both the experimental and theoretical sides. To investigate intrinsic quantum phenomena and achieve desired functionalities, it is important to fully understand the charge transport characteristics of single-molecule devices. In this Review, we present the principles that have been developed for fabricating reliable molecular junctions and tuning their intrinsic properties from an engineering perspective. Through holistic consideration of the device structure, we divide single-molecule junctions into three intercorrelated components: the electrode, the contact (spacer–linker) interface and the molecular backbone or functional centre. We systematically discuss the selection of the electrode material and the design of the molecular components from the point of view of the materials, the interface and molecular engineering. The influence of the properties of these elements on the molecule–electrode interface coupling and on the relative energy gap between the Fermi level of the electrode and the orbital energy levels of the molecule, which directly influence the charge transport behaviour of single-molecule devices, is also a focus of our analysis. On the basis of these considerations, we examine various functionalities demonstrated in molecular junctions through molecular design and engineering.

The physical limitations of the miniaturization of Si-based electronic devices^{1,2} motivate a growing interest in single-molecule electronics, a field being focused on by scientists with expertise spanning chemistry, materials science, physics, electronics and engineering. The field dates back to 1974, when Ratner and Aviram first proposed that a single molecule with an electron-donating group and an electron-withdrawing group at opposite ends could behave as a rectifier³. With developments in both experiments and theory, this topic has become a burgeoning subfield of nanoscience and has begun to develop beyond the basic description of carrier transport and to expand in different research directions, reflecting the interdisciplinarity of the field^{4–9}.

Several approaches to building and studying molecular junctions have been developed^{4,10}, including mechanically controllable break junctions (MCBJs)^{11–13}, conductive atomic force microscopy^{14,15}, electromigration^{16,17}, scanning tunnelling microscopy (STM) break junctions^{18,19}, on-wire lithography²⁰, oxidative lithography^{21,22} or methods based on self-aligned templates²³, thermally deposited metal films²⁴, mercury drop electrodes^{25,26} or large-area molecular junctions²⁷. These sophisticated techniques enable the probing of charge transport at the molecular level^{28–31}. Because

charge transport in single-molecule junctions is quantum mechanical in essence, molecular electronics also offers unique opportunities for the discovery of fundamental physical phenomena and for the direct observation of effects that are not accessible in bulk materials studied with traditional approaches. These effects include quantum interference (QI)^{32–34}, the Coulomb blockade¹⁶ and the Kondo effect^{16,17}. Moreover, devices with various remarkable functionalities — for example, single-molecule switches^{35–38}, molecular thermoelectronic devices^{39,40}, molecular diodes^{5,41}, molecular spintronic devices^{42,43} and sensors with single-molecule sensitivity^{44–47} — have been realized within molecular junctions.

Over the past two decades, single-molecule electronic systems have matured into a platform that enables the study of fundamental properties of materials at the molecular or atomic level, in particular their charge and quantum transport characteristics, including the energy gap between the Fermi level of the electrode and the energy levels of the molecular orbitals, the electrode interface coupling and the intrinsic functions of molecules^{4–6,28,29,32,48–53}. To realize precise control of these effects and to construct robust molecular junctions, it is helpful to start from a holistic analysis of the

¹Beijing National Laboratory for Molecular Sciences, State Key Laboratory for Structural Chemistry of Unstable and Stable Species, College of Chemistry and Molecular Engineering, Peking University, Beijing, China.

²Department of Chemistry, Northwestern University, Evanston, IL, USA.

³Department of Chemistry, University of Pennsylvania, Philadelphia, PA, USA.

*e-mail: stoddart@northwestern.edu; guoxf@pku.edu.cn

<https://doi.org/10.1038/s42254-019-0022-x>

Key points

- Single-molecule electronics has become a burgeoning subfield of nanoscience and has begun to develop beyond the basic description of carrier transport, expanding in different research directions.
- A single-molecule junction can be divided into three intercorrelated components: the electrode, the contact interface and the molecular backbone or functional centre.
- Both the mechanical stability and electronic coupling of the molecule–electrode interface increase with the binding energy of the electrode–anchoring moiety interaction. A compromise between these factors can be achieved by inserting suitable spacers between the molecular kernel and anchoring groups.
- To select suitable electrode materials, chemical inertness to air, good processability, suitable work function and good compatibility with molecules should be taken into consideration.
- The structures of molecular bridges can be tuned by the molecular length, the geometry of the main chains, the responsiveness of the functional centres and the types of side groups, offering opportunities to probe intrinsic physical properties and realize various functionalities.
- Challenges in the field of single-molecule electronics include improving device-to-device uniformity, stability, integration capability and accuracy of theoretical models.

structure of single-molecule junctions, which consist of three intercorrelated components: the electrode, the contact interface and the molecular backbone or functional centre (FIG. 1). In this Review, we examine in detail these three components from an engineering perspective. This in-depth discussion is supplemented with a survey of important achievements in the application of single-molecule junctions to establish structure–function relationships. We conclude by outlining the crucial issues that will need to be solved to enable the successful development of next-generation, single-molecule optoelectronic devices for industrial applications.

Interface engineering

Interface coupling is one of the most critical factors influencing the properties of optoelectronic devices, such as solar cells and organic or polymer optoelectronic devices. In the study of single-molecule electronic devices, optimal interface engineering is also a focus of research (BOX 1) and the most challenging issue that hampers the development of reliable molecular junctions. It was statistically proved that through-bond electrical contacts to octanedithiol monolayers are at least four orders of magnitude more conductive than physical contacts, emphasizing the key role of chemically bonded contacts in the measurement of intrinsic molecular properties¹⁴. The ideal interface between single molecules and the leads would be well defined, stable and highly conducting. Although notable efforts have been made towards this end, achieving the ideal molecule–electrode interface remains a formidable challenge.

Anchoring groups

Chemical synthesis offers many possibilities for optimizing the interface by tailoring the anchoring groups, which are the key to the mechanical stability of contacts and control the electronic coupling between molecules and electrodes. Molecular topologies have a direct effect on the transport mechanism and its efficiency. Indeed, the anchoring groups affect the charge injection

barrier and the molecular orbitals, which are the pathways for electron tunnelling. The injection energy — the energy offset between the Fermi level of the electrode and the energy level of the molecular orbitals dominating the conductance (usually the highest occupied molecular orbital, HOMO, or the lowest unoccupied molecular orbital, LUMO) — is an important parameter to control.

Because studies of single-molecule charge transport are often based on nano-gapped gold electrodes, in this section, we focus our discussions on the interactions between anchoring groups and gold electrodes. According to the nature of the bonds between anchoring groups and Au atoms, anchoring groups can be divided into two kinds: covalent bonding groups and donor–acceptor bonding groups. Generally speaking, the interfacial electronic coupling achieved with covalent bonding is more efficient than that obtained with donor–acceptor bonding as a consequence of the higher bonding strength.

For covalent bonding, the thiol group (–SH) was the first and is currently the most widely employed anchoring group owing to its high binding energy and high probability of junction formation. However, multiple bonding scenarios are possible for Au–S covalent bonds and for the formation of Au–SH donor–acceptor bonds, resulting in a wide range of single-molecule conductance characteristics^{70–75}. Another candidate for strong interface coupling is the covalent Au–C (*sp*) bond, which is established by either extrusion of a trimethyltin moiety or by post-deprotection of a trimethylsilyl moiety^{76–79}. Compared with thiol anchoring groups, Au–C (*sp*) bonds lead to stronger hybridization of the molecular and metal states and to a more distinct energy shift of the peaks towards the Fermi energy, E_F . This can be attributed to the hybridization of the molecular orbitals with the leads. As a result, molecular junctions with Au–C bonding exhibit improved mechanical stability and high electrical conductivity. Moreover, the conductance variations of Au–C bonds are substantially reduced owing to the more stable bonding configuration (top position).

Donor–acceptor bonding involves electron transfer from either π -donors or lone pair donors to Au atoms. Commonly used π -donors include fullerenes^{80,81} and other aromatic rings such as pyrene^{82,83}. Most anchoring groups based on lone pair donors are general σ -donor ligands, similar to those found in coordination chemistry. Typical π -donor and lone pair donor anchoring groups are listed in TABLE 1. It has to be noted that donor–acceptor bonding results in a narrow conductance distribution in single-molecule junctions because of selective binding to undercoordinated adatoms on the surface of the gold electrode, which limits the Au–anchor geometry.

Au–N bonding has been widely used in single-molecule junctions. Among the three N-donor anchoring groups (TABLE 1), the stability is reported as pyridine > amine > nitrile, whereas the binding energy follows the sequence pyridine > nitrile > amine⁷⁵. In addition to the lone pair donation from the N atoms, the delocalized π -character of pyridine and nitrile also contributes to the binding energy^{18,84,85}. The low binding

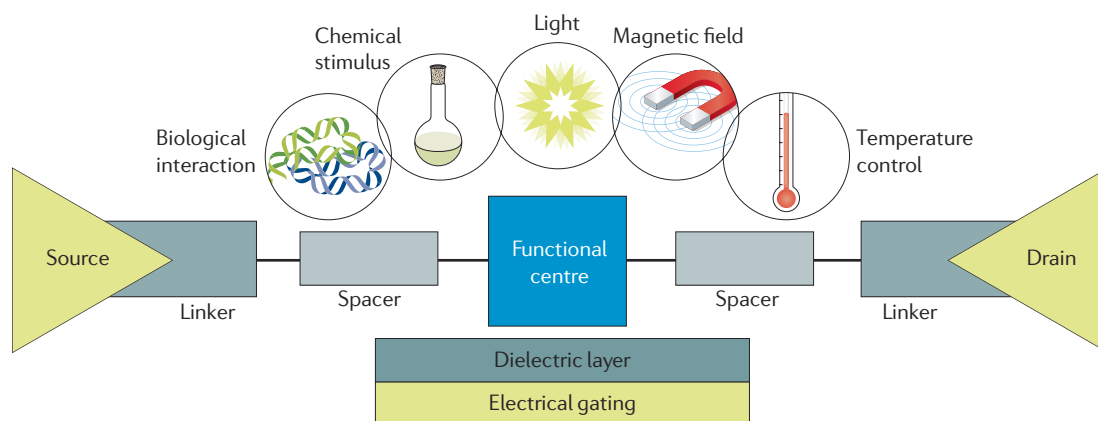


Fig. 1 | **Structure of single-molecule junctions.** The schematic highlights the electrodes (yellow), contact interface (including the linker, dark grey, and the spacer, light grey) and functional molecular centre (blue). Various molecular junctions can be obtained by designing functional molecular bridges that respond to external stimuli, such as biological interactions, chemical stimuli, light, magnetic or electric fields and temperature.

energy of amines can be attributed to the steric hindrance that is induced by the H atoms bonded to the N atom^{75,82,86}. Because the Au–amine bond is not highly oriented, the formation of molecular junctions is unconstrained by the contact structure and is, in principle, straightforward^{71,74,87,88}. The poor stability of the Au bond with nitrile is a result of its long and stiff structure, which prevents effective coupling with the molecular kernel. For nitrile, short biphenyl molecular junctions have been shown to be in two contact geometries with similar binding energies: one is a linear C–N–Au bond with a low-coordination-number Au atom; the other is attached to a ‘terrace-type’, high-coordination-number Au atom with an assumed C–N–Au angle of $\sim 160^\circ$ (REF.⁸⁹).

For more complex anchoring groups, the stability and conductivity both follow the sequence Au–NH₂R < Au–SMeR < Au–PMe₂R (REFS^{70,72,90}), which can be attributed to several factors. The σ -donation from lone pairs to metal atoms follows the sequence phosphines > amines > sulfides. Moreover, the π -backdonation from metal atoms to the ligands is more prominent in phosphines and sulfides than in amines. The enhanced availability of *d* states in sulfides and phosphine ligands affords a π -channel pathway for electron transport through SMe-bridged and PMe₂-bridged molecular junctions. The additional π -channel can explain the conductance differences. The shape and size of lone pair orbitals also have an effect on the stability: larger and more diffused orbitals lead to higher tolerance of bonds to junction stretching. As a result, in a step-length histogram, the length steps of the SMe ligand are substantially longer than those of the NH₂ ligand, although their bond strengths are roughly equal⁹⁰.

Recently, molecular junctions using NCS and NCSe as anchoring groups have also been established, exploiting the excellent affinity of S and Se towards Au (REFS^{76,79}). These experiments indicated that replacing S with Se facilitates the orbital interactions between the Au electrode and the anchoring group and enhances the stability of the junction. Owing to its large molecule–metal interface and affinity to precious metals, fullerene has also been widely employed as an anchoring group.

Indeed, fullerene moieties can induce a shift of the restrictive barriers for electron transfer from the molecule–metal contact interface to the molecular core, resulting in straightforward charge injection in the molecular kernel^{80,81}.

Contact stability

To date, several strategies have been proposed to improve the contact stability and electronic coupling. One approach is to enhance the stability of electric contacts by interconnecting multipodal (bipodal or tripodal) anchoring groups at the end of the molecular kernel (FIG. 2a)^{91–93}. Another strategy is to improve electron delocalization in the anchoring groups to increase the number of coupling conduction channels at the contact interface. The carbodithioate group (–CS₂H)^{94,95} is a good candidate, as it has two S atoms at the end and a delocalized *p*-conjugated electronic structure, which can interact with Au leads through double-bonded S. Notably, the *s* and *p* orbitals of carbodithioate groups (CS₂) can hybridize with the *d* orbitals of Au to generate an additional coupling pathway mediated by the *p* orbitals for electron transport. As a result, carbodithioate-bridged molecular junctions provide substantially improved conductivity in comparison with traditional thiol-linked molecular junctions, owing to the increased electronic coupling and reduced electron transport barrier. The dithiocarbamate group (–NCS₂H)⁹⁶ has also been employed to develop optimized electrical contacts for single-molecule junctions. As in the carbodithioate group, the *s* and *p* orbitals on the CS₂ moiety of dithiocarbamate (NCS₂) can hybridize with the *d* orbitals of Au atoms, whereas the non-bonding electron pair on the N atom can increase the delocalization and strength of Au–S antibonds, which are induced by the hybridization of thiolate frontier orbitals (S 3*p* orbitals) with the *d* and *s* orbitals of Au atoms. The electron-donating effect of the N lone pair can also reduce the injection gap between the Fermi level of the electrode and the HOMO. As a result, the delocalized electronic states of dithiocarbamate anchoring groups bonded to Au electrodes lead to a reduction in the contact resistance by two orders of

magnitude as compared with thiolates on Au and to a stable molecular junction⁹⁶.

Spacers

Overly strong interface coupling may trigger detrimental effects (BOX 1), including the loss of intrinsic functionalities of single molecules and poor gating effects in three-terminal structural devices. By contrast, both the mechanical stability and electronic coupling increase with the binding energy between the electrode and the anchoring moiety, as mentioned above. Hence, a compromise between mechanical stability and electronic coupling is required to optimize the interface. This may be achieved by inserting methylene groups between the molecular kernel and anchoring groups as spacers.

By effectively cutting off the π -electron delocalization, methylene groups can substantially decouple electronic interactions between the molecular functional centre and the electrodes while maintaining strong mechanical contacts. Nevertheless, few attempts have been made to control interfacial coupling by using this method.

The effect of spacers on quantum transport was investigated¹⁶ in three-terminal single-molecule transistors fabricated by electromigration. Specifically, two related molecules having a Co ion bonded to polypyridyl ligands in turn linked to insulating tethers (methylene groups) of different lengths were studied (FIG. 2b). The coupling strength between the ion and the electrodes could be effectively tuned by altering the number of methylene groups. Devices based on molecules with

Box 1 | Interface coupling between molecules and electrodes

In the absence of inelastic interactions, the current in single-molecule junctions is given by the expression^{54–57}:

$$I = \frac{2e}{h} \int_{-\infty}^{\infty} T(E) [f_L(E) - f_R(E)] dE$$

where $T(E)$ is the electron transmission probability as a function of energy, E ; e is the electron charge; h is Planck's constant; and $f(E)$ is the Fermi distribution function (the subscripts L and R refer to the left and right electrode, respectively). It is assumed that a single molecular orbital located at an energy E_0 from the Fermi energy E_F is coupled to the right and left electrode in the way illustrated in the single-level model in the figure, which results in level broadening and (disregarding possible energy dependence of the corresponding self-energy) yields a resonance in the transmission function with a Lorentzian shape:

$$T(E) = \frac{4\Gamma_L\Gamma_R}{[E - E_0]^2 + [\Gamma_L + \Gamma_R]^2}$$

where Γ_L and Γ_R are the coupling constants with regard to the right and left electrodes, respectively. The coupling strength at the molecule–electrode contact interface and the injection gap (the energy offset between the dominant conducting molecular orbitals and the electrode's Fermi level) are the two determinant factors. The conductivity of single-molecule junctions increases with the interface coupling strength and decreases with the injection gap. At equilibrium, the efficiency of molecular states as conducting channels is determined by the contact symmetry and by the degree of molecule–electrode orbital overlap, whereas the coupling-induced charge and potential perturbation produce a shift in the molecular levels relative to the electrode's Fermi level⁵⁸.

The degree of molecule–electrode orbital overlap is quantitatively described by the interface coupling. In the case of weak interface coupling, the broadening of the molecular energy levels is small. As the interface coupling becomes stronger, the broadening of the energy levels increases. When the broadening is large enough, the properties of the original molecular orbital are essentially lost⁵⁹, along with the intrinsic functionality of the molecule^{60–63}. In addition, the charge transport mechanisms in three-terminal devices are influenced by the strength of the interface coupling.

Correspondingly, various phenomena could be observed in differential conductance maps as a function of the source–drain voltage and gate voltage. Interested readers can find more details in specialized articles^{6,30,64}.

For the alignment of orbital energy levels, the picture is not as clear as for the energy level broadening. The factors affecting the coupling are complex. In general, two mechanisms have been proposed on the basis of theoretical and experimental investigations and are consistent with the observations on self-assembled monolayer semiconductor devices. The first mechanism involves the interfacial dipole that is formed owing to partial charge transfer between the orbitals of the molecule and electrode, which affects all molecular orbitals in a similar way, shifting them in the same direction (up or down)^{7,65,66}. By contrast, the other mechanism is transport gap renormalization, whereby the occupied levels migrate upwards and the unoccupied ones migrate downwards in energy. This phenomenon can be attributed to the formation of image charges in the electrodes owing to the movements of electrons (either added to or removed from the molecules). In both regimes, the shift in molecular energy levels is positively correlated with the strength of the interface coupling^{6,7,13,67–69}. In the transport gap renormalization regime, the shift increases with the electrode density of states at the Fermi level. For a clearer and more unified view of the sequence of orbital energy levels, additional efforts are needed to understand the competition between these two regimes. HOMO, highest occupied molecular orbital; LUMO, lowest unoccupied molecular orbital.

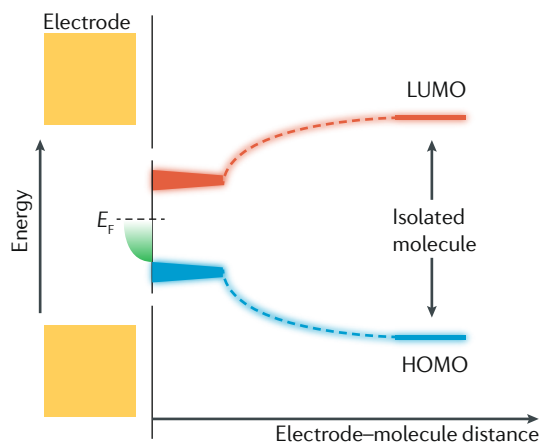
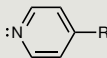
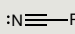
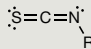
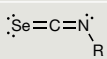
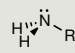
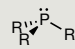
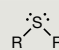
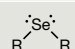

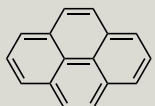


Table 1 | Typical anchoring groups for donor–acceptor bonding

Type of donor	Structure	Name
Lone pair donors		4-Substituted pyridine
		Nitrile
		Organothiocyanate
		Organoselenocyanate
		Primary amine
		Tertiary phosphine
		Thioether
		Selenoether
π -donors		C ₆₀
		Pyrene

Adapted from REF.⁶, Springer Nature Limited.

insulating tethers (weak interface coupling) showed a Coulomb blockade — a single-electron phenomenon occurring when the charging energy needed to move a single electron through a system exceeds the available energy, with potential applications in low-power and fast devices — owing to the presence of the Co ion island. By contrast, devices based on molecules without insulating tethers (intermediate interface coupling) presented a Kondo resonance, an increase in the conductance at low bias arising from the formation of a many-body singlet state caused by the scattering of conduction electrons in the metal electrodes on a local spin on the Co ion island. The interest in the Kondo effect lies in the fact that it is regarded as the simplest manifestation of the interaction of localized electrons with delocalized electrons, which is a question central to many problems in solid-state physics. Relatively weak coupling is also needed to conserve the QI effect, as was observed in a study of charge transport in benzene molecules bearing different numbers of methylenes at the *meta* positions of the anchoring groups⁹⁷.

A series of single-molecule photoswitches based on diarylethene derivatives with different molecular structures (FIG. 2c) was proposed^{35,60}, employing two strategies to effectively weaken the electronic coupling between the graphene electrodes and the diarylethene functional centre. One approach is to insert methylene groups between the diarylethene functional centre and the anchoring groups; the other consists in introducing

electron-withdrawing groups in the diarylethene functional centre, for example, by substituting the hydrogenated cyclopentene in molecule I-1 by the fluorinated unit in molecules I-2 and I-3. The interface coupling strength Γ of graphene–molecule I-4 molecular junctions is much lower than those of the other three molecules ($\Gamma_{I-4} < \Gamma_{I-3} < \Gamma_{I-2} < \Gamma_{I-1}$). Thus, only molecule I-4 achieves stable and reversible photoswitching, whereas the other three molecules exhibit unidirectional photoswitching (from open and non-conducting to closed and conducting diarylethene) as a consequence of the strong interface coupling that induces energy and electron transfer from the photoexcited molecule to the extended π -electron conjugated system in the graphene electrodes.

In addition to controlling the interface electronic coupling and mechanical stability of molecular junctions, anchoring groups also affect the energy levels of frontier molecular orbitals, which are determined by the electronegativity of the anchoring groups. Anchoring groups such as amine and thiol usually increase the energy of the frontier molecular orbitals owing to their electron-donating nature. Therefore, in SH-bound and NH₂-bound molecular junctions, hole transport dominates transport, which happens mostly along the HOMO, the orbital closest in energy to the Fermi level of the electrode^{71,74}. By contrast, charge transport in molecular wires bearing electron-withdrawing groups such as pyridine and nitrile is preferentially governed by the LUMO^{84,89,98}. Further work will be needed to elucidate the intrinsic physical principles of interface coupling and the role of interface physics in determining the interfacial electronic structure and in tuning the charge transport characteristics.

Electrode materials

The electrode material is another key factor influencing the injection barrier and interface electronic coupling. To select suitable electrode materials, several factors must be taken into consideration: chemical inertness to air, good processability, suitable work function and good compatibility with organic or biological molecules. Currently, metal-based and carbon-based nanomaterials are widely employed as electrode materials.

Metal electrodes

Among metals, Au is commonly used in molecular junctions, because it meets most of the requirements above. Some other metals (such as Ag, Pt, Pd and Cu) have also been used as electrode materials for molecular junctions. Au, Ag, Pt, Pd and Cu are different from each other in terms of the work function, which in general results in different injection energies. Nevertheless, it has been reported that the injection barrier is independent of the work function and varies for conjugated and saturated systems^{99,100}. The alignment of the molecular energy levels and the interface electronic coupling at the metal–organic contacts are also determined by subtle local interactions (rather than following simple rules), in which the density of states of the metal at the Fermi level has a key role.

Unlike Au, Ag and Cu, Pt and Pd are group 10 elements and thus have stronger *d*-orbital character and a

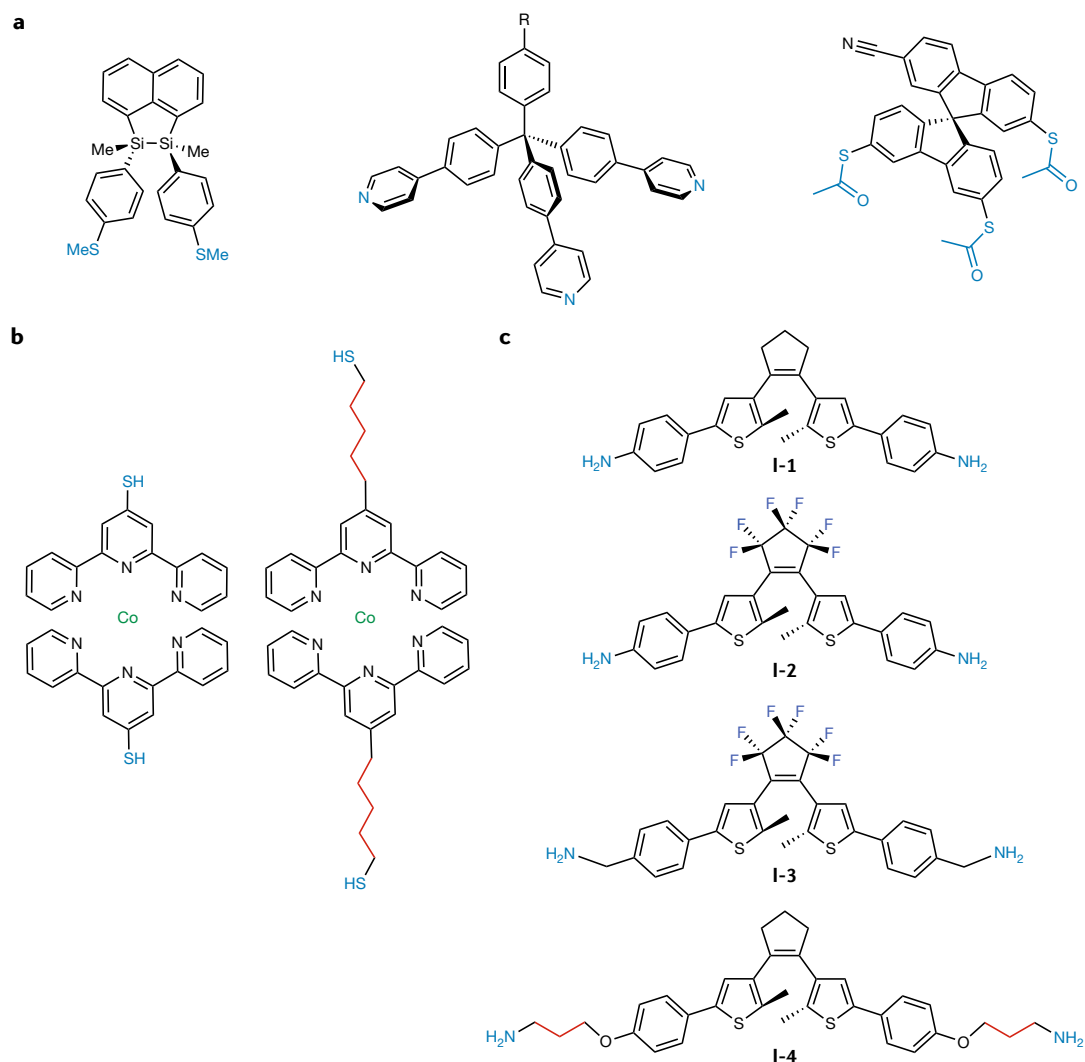


Fig. 2 | **Strategies to control interface coupling.** **a** | Multipodal anchoring groups at the end of the molecular kernel can provide a sufficient number of stable electric contacts, improving the contact stability (chemical structures from REFS^{91–93}). **b** | Transition metal complexes with different numbers of methylene groups (zero or five) connecting a Co ion island with the anchoring groups (chemical structures from REF.¹⁶). **c** | Diarylethene derivatives designed by inserting methylene groups or electron-withdrawing groups to control interface coupling (chemical structures from REFS^{35,60}).

larger local density of states near the Fermi level. By contrast, Au presents enhanced d states owing to the higher position of the d band edge (reflecting known relativistic effects). In general, the π -character of the bonds formed by Pt and Pd provides an alternative channel for electron transfer, resulting in superior conductance.

A study of isothiocyanate-terminated alkanes¹⁰¹ revealed that the conductance of Pd and Pt junctions was 2–3-fold higher than that of Au junctions, despite the fact that Au and Pd have almost identical work functions. The d band of metals has the right symmetry to couple with isothiocyanate π -orbitals near E_F , and the relatively enhanced d character at E_F of Pd and Pt increases the metal–molecule d - π interactions. The role of the d orbital was also demonstrated in oligoacene-based molecular junctions³⁹. A strong hybridization between the Pt frontier orbitals and the dominant conducting molecular orbitals induces a smearing of the molecular features, yielding a large plateau of high transmission. By contrast,

in Ag–oligoacene-based molecular junctions, the transmission is mostly controlled by the hybridization of the valence s -orbitals of Ag atoms with the molecular π -orbitals, and the junctions maintain the molecular level character owing to a small contribution from d orbitals around E_F . Another study revealed that the value of 4,4'-bipyridine conductance peaks is an order of magnitude lower when Ag electrodes are used rather than Au electrodes⁹⁹. This difference can be attributed to reduced d - π^* hybridization, as well as to a lower metal–molecule coupling caused by the weaker d_{yz} -orbital character of the density of states of Ag at E_F . Unlike Au and Ag, Cu forms a short atomic wire during the elongation of the junctions, leading to fewer adsorption sites available on the wire surface and to a relatively sharp peak in conductance histograms^{102–104}.

Magnetic metals such as Ni (REFS^{105–107}) and Fe (REF.¹⁰⁸) have also been used as electrodes in molecular junctions. Owing to spin-polarized orbital hybridization at the

Fermi level of the electrode, interesting magnetic phenomena such as the gate-controlled Kondo effect¹⁰⁹, which allows the precise control of the spin degree of freedom, providing information on the junction and holding promise for device applications, have been observed.

Carbon-based electrodes

Nevertheless, the applicability of metallic materials is limited by atomic mobility and incompatibility with single molecules in terms of size and work function. Carbon-based nanomaterials such as carbon nanotubes and graphene may be considered as alternative electrode materials for molecular electronics¹¹⁰. In particular, graphene is regarded as a viable candidate for the post-complementary metal oxide semiconductor (CMOS) electronics era, because high-quality monolayers of graphene can be grown at the wafer scale by using chemical vapour deposition. More importantly, graphene is atomically stiff and compatible with single molecules owing to its simple chemical composition and atomic bonding configuration, arising from its sp^2 -hybridized carbon atoms arranged in a honeycomb lattice. Patterning at the nanometre scale to create point contacts has been achieved in graphene by electron-beam lithography²⁵ or electroburning¹¹¹. Reliable room temperature molecular orbital gating has been demonstrated in graphene–molecule–graphene junctions^{111–113}, which is impossible in metal–molecule–metal junctions owing to gate screening by the thick electrodes. These efforts have the advantage of bringing single-molecule electronics into a domain in which the junction dimensions are shrunk to two dimensions. Another merit of carbon-based electrodes is the contact flexibility, as the contact can be in either a covalent bonding or π – π stacking configuration. When molecules are covalently attached to graphene directly via anchoring groups, the electronic structure can be extended to the functional molecular kernel, making low-ohmic contacts possible^{25,112,114}. Furthermore, an improved value of the contact resistance, of the order $\sim 100\text{ k}\Omega$ per 20 nm^2 , was obtained by exploiting a weak π – π stacking interaction¹¹¹ that can be realized only with broad contact areas.

Increasing attention has been recently paid to other semiconductor materials that can be used as electrodes in single-molecule junctions. Among CMOS-compatible materials, Si (REF.¹¹⁵) and GaAs (REFS^{116,117}) are ideal candidates for the study of charge transport through single-molecule junctions. In comparison with metallic materials, the Fermi levels of these materials can be readily tuned, providing alternative approaches for the integration of novel functionalities into molecular junctions.

Molecular engineering

The structures of the molecular bridges at the core of molecular electronic devices are extremely diverse, offering the opportunity to probe the intrinsic relationships between the structure of a molecule and its physical properties (such as switching, thermal conductivity, rectification, spin transport and QI) and to install various functionalities through the precise design and

engineering of the molecular structures. Parameters that can be tuned by flexible organic synthesis include the length of the molecules, the geometry of the main chains, the responsivity of functional centres and the type of side groups. In this section, the strategies developed for creating functional molecular devices are reviewed from the molecular engineering point of view, with the aim to distil some general principles for the rational design of single-molecule junctions.

Donor–acceptor asymmetry

Rectification is mainly induced by a structural asymmetry in molecular junctions or in the spatial profile of the electrostatic potential. For example, contact asymmetry is an efficient strategy for realizing the rectifying effect and was used to achieve rectification ratios in excess of 200 (REF.¹¹⁸). Another widely investigated approach is to use different electrode materials^{117,119–122} or design different anchoring groups^{123,124}. From the molecular engineering point of view, rectification is still understood in the context of the Aviram–Ratner model, originally proposed in 1974 (REF.³), which is based on asymmetric donor–bridge–acceptor (DBA) molecules. The asymmetry here refers to the fact that electron transport from the acceptor to the donor molecule is favoured, because a transition from the excited D^+BA^- to the ground D^0BA^0 is energetically favourable (FIG. 3a). Specifically, electron transport through a molecule involves three tunnelling steps, with the electron moving from the electrodes through the LUMO of the acceptor unit and the HOMO of the donor unit, which respond differently to the electric field between the electrodes upon application of a bias voltage. Under a forward bias, these two levels become closer in energy and align in the bias window (and vice versa). Notably, the bridge can be a σ -bond or a π -bond, or there can be no bond at all. The judicious design of the strongly electronegative and electropositive substituents, as well as the optimization of the interface coupling, is key to the improvement of the rectifying properties of molecular junctions. However, rectification has been achieved in only a few cases^{41,125–128} by using asymmetric molecular structures, owing to the challenging chemical synthesis (FIG. 3b). The performance of these systems is still far from that of bulk devices⁵.

Molecular length

The molecular length is an important factor in the control of single-molecule conductance and has been extensively investigated in various molecular systems. First, it determines the distance that charges need to travel between the right and left electrode, thus affecting the single-molecule conductance. There are two distinct mechanisms of charge transport: coherent tunnelling independent of temperature and temperature-dependent incoherent hopping. Coherent tunnelling dominates in short molecules (usually $<4\text{ nm}$), whereas in an off-resonant situation, the molecular conductance decreases exponentially with the molecular length^{129,130} as $G = G_0 \exp(-\beta L)$, where G is the molecular conductance, G_0 is an effective constant conductance, L is the molecular length and β is

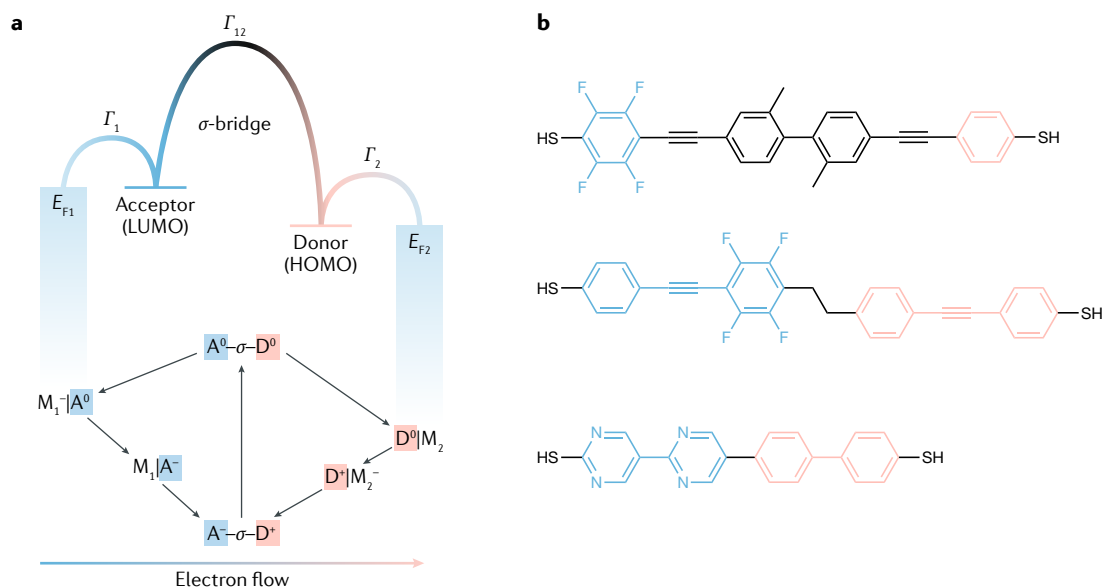


Fig. 3 | **Single-molecule diodes.** **a** | Energy diagram of Aviram–Ratner rectification in a single-molecule device, showing that electrons can flow from the acceptor (A) to the donor (D) molecule more easily than from D to A because the barrier of a transition from the excited D^+BA^0 state to the ground D^0BA^0 state is lower. M represents the molecule in different states, and Γ represents the coupling between the different parts of the junction (chemical structures from REFS^{41,126,127}) **b** | Examples of asymmetric molecular structures that have been used to realize single-molecule diodes (chemical structures from REF.¹²⁸). E_F , Fermi energy; HOMO, highest occupied molecular orbital; LUMO, lowest unoccupied molecular orbital.

the decay constant. Incoherent hopping is believed to be responsible for carrier transport through long molecular wires. In Marcus theory, which explains the rates of electron transfer¹³¹, the conductance obeys an Arrhenius relation, $G \propto \exp(-E_A/k_B T)$, where E_A is the hopping activation energy. Carrier hopping is characterized as a weak length-dependent process that influences the conductance, making it inversely proportional to the molecular length. The charge transport mechanism changes from tunnelling to hopping with increasing molecular length¹³. Here, we focus on single-molecule properties, instead of discussing molecular assemblies that are more complex to describe owing to intermolecular interactions. Because there have been only a few studies investigating the length-dependent hopping transport mechanism, we mainly discuss coherent tunnelling in different oligomeric backbones.

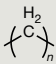
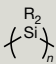
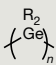
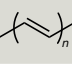
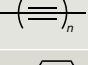


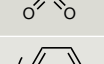
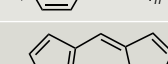
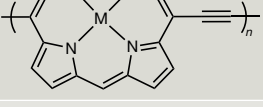
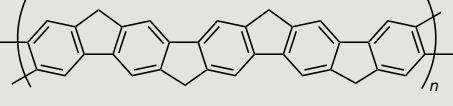
β -Quantitatively describes the ability of different oligomeric kernels to transport charge carriers and is mainly determined by the degree of conjugation between repeated units. β -Can also be affected by anchoring groups^{132,133}, spacers¹³⁴ and by the solvent environment¹³⁵, most likely because of variations in the alignment of the Fermi level of the electrode within the HOMO–LUMO gap of the molecule and of charge transfer at the molecule–electrode interface. The mediation of long-range charge transport by the molecule degrades as the β -value increases. Indeed, the β -values of π -conjugated molecules are typically lower than those of aliphatic σ -bond molecules. π -Conjugated molecules can also function as highly conductive wires by virtue of the delocalization of the molecular orbitals and the small energy gap between

the HOMO and LUMO. Typical β -values for different oligomeric materials are summarized in TABLE 2. Owing to the lack of delocalized charges, the β -value of alkanes is the highest ($\sim 0.94 \text{ \AA}^{-1}$)¹³⁶. Despite the similar σ -bond structure in alkanes, silanes and germanes, the β -value decreases as the number of atoms increases. These conductivity trends arise from delocalization in the Si–Si and Ge–Ge σ -bonds — the same delocalization that makes Si and Ge excellent bulk semiconducting materials⁵².

π -Conjugated molecular backbones tend to have lower β -values owing to effective charge delocalization. For alkenes¹³⁷ and alkynes⁷³, the spatial distribution of π -electron clouds is in the plane of the molecular backbone owing to the unique conformation of the backbone, and this results in more effective conjugation. Hence, alkenes and alkynes are better at mediating long-range charge transport than *p*-phenylenes^{138,139}. In the quest to realize a larger degree of electron delocalization, several strategies have been proposed: using more electron-rich structures, such as thiophenes^{140–142} and metalloporphyrins^{143,144}; locking the conformation of repeated units in the same plane to maximize the degree of conjugation^{146,147}, as in cyclopentadifluorenes; and inserting alkynyl linkers between the repeated units to promote electronic conjugation along the oligomer, as in metalloporphyrins^{144–146}.

Additionally, in conjugated oligomeric molecules, the HOMO–LUMO gap decreases as the molecular length increases, altering the injection energy. Length-dependent thermoelectricity has been observed in several oligomeric backbones^{138,140}, but there is not such a clear trend for length-dependent conductance. This deficiency may be attributed to the fact that thermoelectricity depends

Table 2 | Conductance is dominated by coherent-tunnelling mechanisms

Oligomeric material	Structure	β (\AA^{-1})
Methylene		0.94 (REF. ¹³⁶)
Silylene		0.39 (REF. ⁵²)
Germylene		0.36 (REF. ⁵²)
Alkenediyl		0.22 (REF. ¹³⁷)
Alkynediyl		0.17–0.32 (REF. ⁷³)
<i>p</i> -Phenylene		0.42 (REF. ¹³⁸)
2,5-Thiophenediyl		0.29 (REF. ¹⁴⁰)
Dioxo-2,5-thiophenediyl		0.20 (REF. ¹⁴²)
<i>p</i> -Phenyleneethynylene		0.20 (REF. ¹⁴⁷)
Metalloporphyrin		0.04 (REFS ^{143,144})
Cyclopentadifluorene		0.21 (REF. ¹⁴⁵)

Adapted from REF.⁶, Springer Nature Limited.

on the characteristics of the molecular orbital that dominates conductance, as well as on the injection energy.

Switchable molecules

By virtue of their potential as building blocks for single-molecule electronics and ultrahigh-density storage devices, functional molecules with bistable or multistable states have been widely studied. Two kinds of conductance switching phenomenon have been observed in single-molecule electronics: stochastic and controllable switching. Stochastic switching results from changes in the molecular states induced by an external electric field or intrinsic vibration effects (often related to temperature)^{4,36}. Here, we focus the discussion on molecular structures with an intrinsic and controllable switching function that promises to advance single-molecule switches towards practical applications. Switches based on three mechanisms have been reported: conformation-dependent switches, electrochemically induced switches and spintronics-triggered switches.

Conformational switches. For conformation-dependent switches, in principle, any molecular species that can isomerize in response to an external stimulus (usually light or the presence of ions) can serve as the core functional centre. The mechanical and conformational stability must be considered, as well as the fatigue resistance. Light stimulation is a commonly used approach to controlling molecular switches and can be integrated into solid-state electronic devices. Photochromic diarylethene derivatives are regarded as ideal candidates for light-driven molecular switches. Upon exposure to light, diarylethene derivatives can reversibly transform between two distinct states with open and closed conformations, a transformation accompanied by substantial changes in the molecular energy levels and electron delocalization but negligible changes in the molecular length. Moreover, diarylethene derivatives (FIG. 2c) have superior thermal stability and fatigue resistance^{148–150}. However, the photophysical properties of individual diarylethenes are sensitive to the environment, and the electrode–molecule contact interface needs to be optimized to attain suitable interaction couplings^{60–62,151,152}. Following almost 20 years of efforts, this challenge has finally been overcome, enabling the realization of fully reversible and stable molecular photoswitches based on single diarylethene molecules with excellent levels of accuracy, stability and reproducibility³⁵. Conductance switching photothermally triggered in situ between two isomers of dimethyldihydropyrene molecules was also demonstrated (ON/OFF ratio, that is, the ratio between the conductances of the two states, is $\sim 10^4$)¹⁵³. Despite its poor fatigue resistance, this molecular structure displayed good mechanical stability (with minimal length change between the two isomers) and good electronic properties.

Electrochemical switches. Redox-active molecules are particularly interesting as switches, because they can be reduced or oxidized by applying an electrochemical gate potential, which permanently changes the number of electrons on the molecule, the energy levels of molecular orbitals and the degree of conjugation, resulting in a switch in conductance. Electrochemical studies of single-molecule conductance focused primarily on organic redox moieties^{154–159} and organometallic compounds^{160–164}. A special group of electrochemical switches, which includes catenanes and rotaxanes, exhibit stereoisomerization, that is, the 3D orientation of atoms in the molecule can change. These switches are mechanically interlocked molecules containing two molecules ‘embracing’ each other. In general, an outer ring can reversibly migrate between two stations (with different electron-donating abilities) of an inner molecule, producing two different conductance states. This switching process is regarded as intermolecular stereoisomerization, because in the first approximation, only one molecule exhibits changes in its position relative to the second molecule. Using this type of molecule, a molecular-scale, 160-kb electronic memory was realized with 10^{11} bits per square centimetre¹⁶⁵.

Electrochemical approaches stabilize charged species, thus facilitating the investigation of the conducting

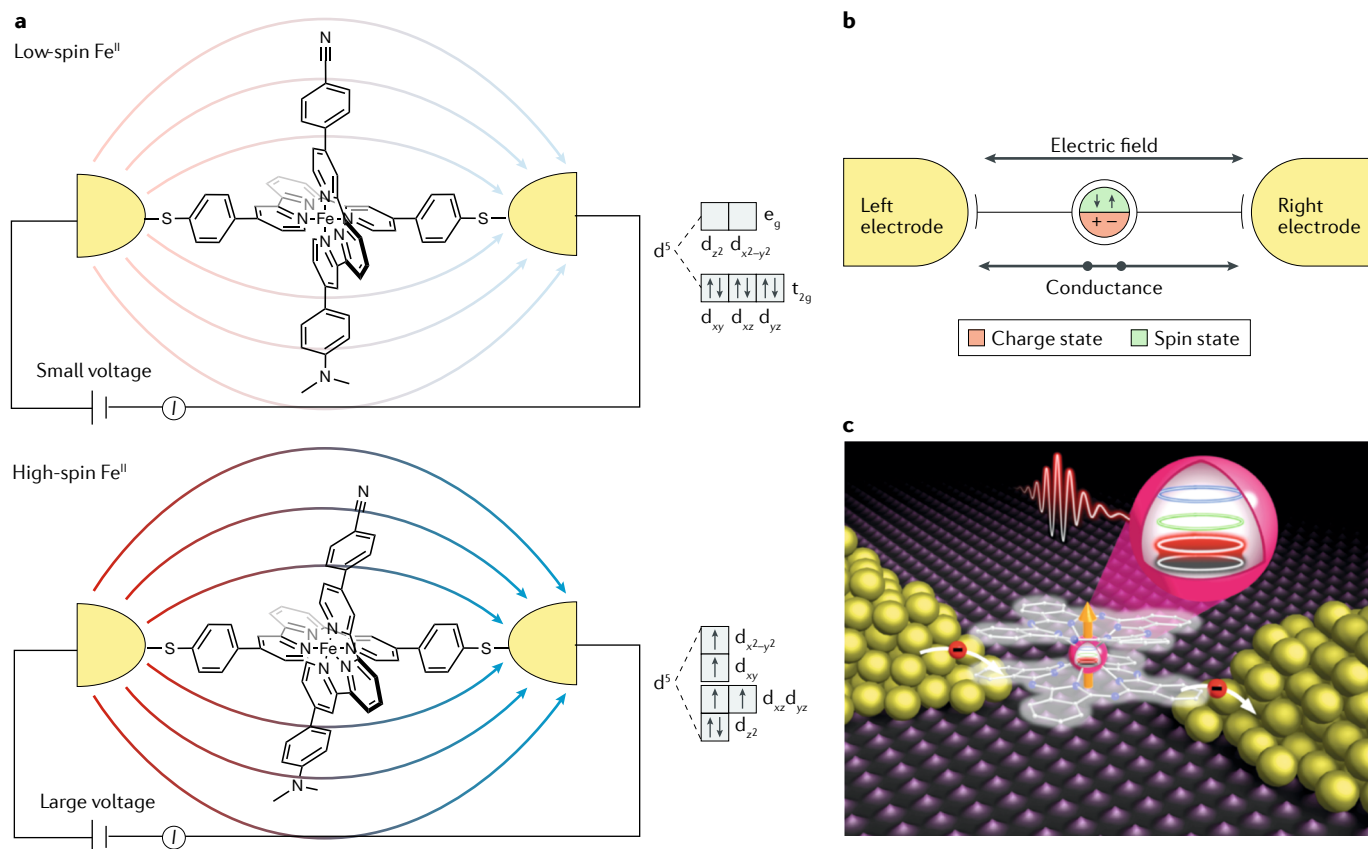


Fig. 4 | **Typical spin-based switches.** **a** | Schematic representation of a spin-based switch with different Fe spin states. Under a small voltage, the Fe^{II} complex sandwiched between the two electrodes is in a low-spin state. When an electric field is applied, the coordination sphere of the Fe^{II} complex is distorted owing to the alignment of the push–pull system, and the system is in a high-spin state. **b** | Spin and charge states of a molecular junction in the presence of the electric field induced by the applied bias voltage. **c** | Schematic illustration of a spin-based transistor based on a single Tb³⁺ ion sandwiched between two phthalocyanine ligands in a Tb–Pc₂ molecular magnet, in which the nuclear spin states of Tb³⁺ (coloured circles) can be manipulated with an electric field pulse (red). e, doubly degenerate; g, symmetric with respect to inversion centre; l, current; t, triply degenerate. Panel **a** is adapted with permission from REF.¹⁷², Wiley-VCH. Panel **b** is adapted from REF.¹⁷³, Springer Nature Limited. Panel **c** is adapted with permission from REF.¹⁷⁰, AAAS.

properties of unstable states, such as radicals^{166,167} and anti-aromatic ions¹⁶⁸. These two kinds of molecules exhibit ON/OFF ratios of ~200 for the radical ion and ~70 for the anti-aromatic ion, whereas oxidized/reduced structures exhibit ON/OFF ratios ≤10. Radical-based and anti-aromatic-based switches are similar in that the big change in the electronic structures occurs after oxidation, as seen in transmission spectroscopy data. This contributes greatly to their high ON/OFF ratios. Despite the absence of general principles guiding the design of electrochemically triggered switches with high ON/OFF ratios, these studies did provide new insight, motivating further work in this area.

Spintronic switches. Spintronics can also be used to achieve switching^{43,169–171}. Different nuclear spin states should lead to different conductance states and could thus be used to encode information or induce switching. The most commonly used molecules in spin-based switches can be divided into two classes: spin-crossover compounds and valence-conversional molecules. Both molecule types have long magnetization relaxation times, and their electronic structures can change

owing to charge rearrangement or atomic relaxation, leading to different states that are electrically readable. Bias-dependent switching was reported¹⁷² in molecular junctions with a spin-crossover coordination compound as the functional centre (FIG. 4a). Molecular junctions based on [Fe^{II}(tpy)₂] complexes were fabricated using the mechanically controllable break junction technique. The Fe^{II} ion changes from a low-spin to a high-spin state at a threshold voltage owing to the distortion of the coordination sphere under a high electric field, resulting in bistability in the current–voltage curves.

Valence-conversional molecules change their valence states as a function of the conductance state or of an applied magnetic field. Voltage-induced conductance switching was demonstrated¹⁷³ in single-molecule, two-terminal break junctions based on a Mo-containing compound, yielding high-to-low current ratios exceeding 1,000 at a bias voltage of less than 1.0 V. This behaviour was attributed to the oxidation of and/or reduction in the Mo ion, mediated by a weakly coupled, localized molecular orbital with a spin-polarized ground state (FIG. 4b). Although the technologically relevant

parameters still have to be determined in real device geometries, these efforts demonstrate the potential of these systems.

Reversible conductance switching was observed¹⁷⁰ also for a Tb^{3+} ion sandwiched between two phthalocyanine (Pc) ligands (FIG. 4c). In this study, a three-terminal nuclear spin qubit transistor fabricated via electromigration and consisting of a Tb–Pc₂ single-molecule magnet was used for electrical transport measurements. By sweeping the magnetic field at constant source–drain and gate biases, the electron spin changed between the $|\uparrow\rangle$ and $|\downarrow\rangle$ states, resulting in a conductance jump. Another reversible switch was realized¹⁷¹ that was based on Ho atoms supported on MgO, with an Fe atom next to the Ho to increase the magnetic field felt by Ho. These studies provide a universal route towards the electrical control of nuclear-spin-based devices by using the hyperfine Stark effect as a magnetic field transducer at the atomic level.

Switches based on quantum interference. Molecular electronic systems exhibit QI (FIG. 5)^{32–34,174–185}. In molecular junctions, the propagation distance of electrons through the devices is comparable to the phase coherent length of the electron wave. Therefore, QI occurs in molecules with quasi-degenerate states (usually two), which are exactly the conducting channels. When partial electron waves propagating through the quasi-degenerate states interfere with each other destructively, the conductance is suppressed; when they interfere constructively, the conductance is enhanced. The phenomenon of constructive QI was observed¹⁷⁷ in a double-backbone junction, which had a conductance larger than that of two single-backbone junctions measured in parallel. One signature of destructive QI in single-molecule electrical circuits is a sharp dip in theoretical transmission spectroscopy plots or in experimental differential conductance plots.

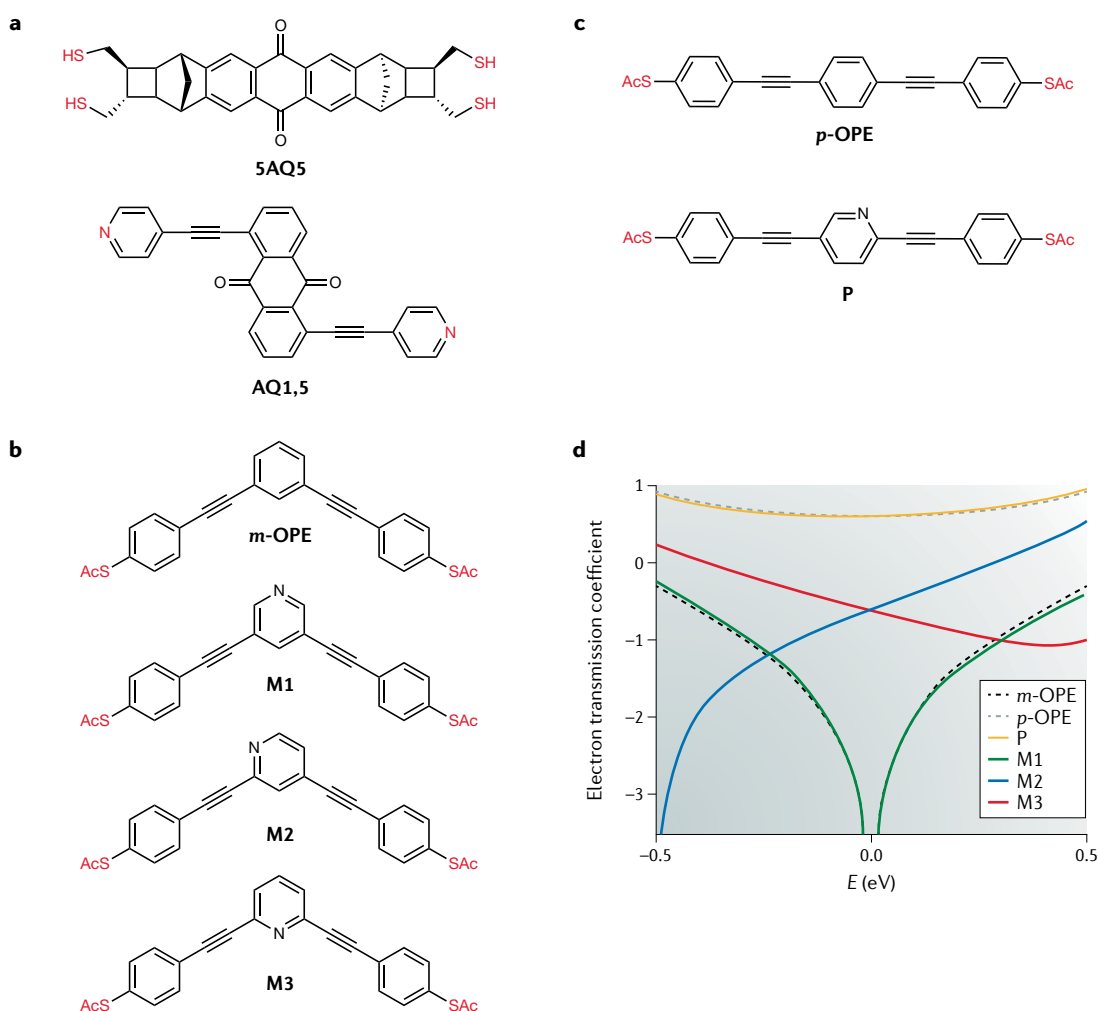


Fig. 5 | **Switches based on destructive quantum interference.** **a** | Two anthraquinone-based molecular structures used for realizing switches based on quantum interference (QI). **b** | Chemical structures of an oligomer with a meta-phenylene ethynylene skeleton (*m*-OPE) and of its derivatives obtained by intercalating a N atom in the middle benzene ring at different positions (M1, M2 and M3). **c** | Chemical structures of a parent compound *para*-OPE (*p*-OPE) and its daughter molecule (P) obtained with N substitution. Chemical structures in panels **a–c** are from REFS^{159,190}. **d** | Corresponding energy (*E*)-dependent electron transmission coefficients, showing the destructive QI effect obtained when the N atom is in a meta position (M1). AQ, anthraquinone. Panel **d** is adapted from REF.¹⁹¹, CC-BY-4.0.

If a destructive QI transmission peak is close to the Fermi level of an electrode, the conductance can be extremely low. This behaviour is attractive because the destructive QI pathway — if it can be switched in a controllable manner — might serve as an ideal OFF state in devices with large ON/OFF ratios. Many theoretical proposals have been put forward for this kind of electrical device, suggesting the application of a gate voltage to regulate the anti-resonance position and/or switch the charge transport pathway between non-QI and destructive QI channels^{186–189}. However, very few experiments have been performed to verify this prediction. QI switches have been constructed^{159,190} on the basis of the electrochemically triggered switching between cross-conjugated anthraquinone (destructive QI) and linearly conjugated hydroanthraquinone (no QI) (FIG. 5a). The ON/OFF ratio exceeded 10. The influence of heteroatom substitutions on QI in single-molecule devices was also investigated¹⁹¹. The conductance changes were induced by modifying a parent oligomer with a *meta*-phenylene ethynylene skeleton (*m*-OPE) by intercalating one N atom into the *m*-OPE backbone to obtain a daughter compound (FIG. 5b). When the N atom was inserted in a *meta* position relative to both acetylene linkers (M1), the daughter's conductance was similar to that of the parent. When the N atom was in a *para* position relative to one acetylene linker and an *ortho* position relative to the other (M2), destructive QI was decreased, and the daughter's conductance was substantially increased (FIG. 5c). When the N atom was in the *para* position relative to both acetylene linkers (M3), the conductance was between those of M1 and M2. By contrast, if the starting structure was connected in a *para* geometry (FIG. 5c), the conductance remained unchanged following N substitution (FIG. 5d). These observations are consistent with theoretically calculated transmission spectroscopy results.

Effect of substituents

Any small variation, electronic or geometric, of the molecular structure in the charge transport pathway can deeply influence the electrical conductance of single molecules. Moreover, changing the atoms or groups at the side-group position, which do not have continuous σ -bonds with the molecular junction, is an effective method to tune the electronic or geometric properties of the molecular backbone and the conductance behaviour. For instance, in the study of 1,4-diaminobenzene-based molecular wires, different substituents were incorporated at the 2-position, 3-position, 5-position and 6-position¹⁹², in which electron-donating groups (such as $-\text{OMe}$ and $-\text{Me}$) and electron-withdrawing groups (such as $-\text{Br}$, $-\text{CF}_3$, $-\text{F}$ and $-\text{Cl}$) made positive and negative contributions to the molecular conductance, respectively. These opposite behaviours originate from the nature of HOMO-dominated charge transport of the amine anchors: substituents that donate electrons to the benzene unit elevate the HOMO energy towards the E_F of Au, whereas substituents that withdraw electrons from the benzene unit stabilize the molecule and decrease the HOMO energy, moving it away from E_F . These observations can be explained in terms of the energy offset between the conducting molecular orbital that is hybridized with

metal electrodes and E_F in the same way that the energy difference between the ground state and the transition state determines chemical reaction rates.

Edge-on chemical modification. An interesting gating effect obtained through edge-on chemical modification in molecular wires (FIG. 6a) was demonstrated¹⁹³ by using a pyridinoparacyclophane (PC) moiety with different substituent groups at the *para*-position of the pyridyl ring, ranging from strongly electron-withdrawing groups to strongly electron-donating groups. The conductance decreases when the substituent changes from a strong donor ($\text{N}(\text{CH}_3)_2$) to a strong acceptor (NO_2 ; FIG. 6b,c). If the compound contains no nitro groups, the charge density on the N atom of the pyridine ring is directly affected by the electronegativity of the substituents. Electron-donating groups increase the negativity of the pyridine ring (and thus of the N atom), resulting in increased conductance by facilitating the hole current through the molecule. If the substituent is changed from an electron donor to an electron acceptor, the charge tunnelling barrier of compounds containing no nitro groups increases (FIG. 6b). For Cl, H, OCH_3 and $\text{N}(\text{CH}_3)_2$ molecules, the HOMO is the dominant molecular orbital, whereas charge transport in nitro compounds occurs through the LUMO orbital, which is exclusively confined in the pyridine group. In this case, charges have to tunnel through the nitropyridine group, degrading the conductance. Regardless of the nature of the substituents, the molecules show similar conductance after protonation by trifluoroacetic acid (FIG. 6c)¹⁹⁴. The effect of protonation is the same as that of the nitro groups: charges tunnel through the LUMO, which suppresses the conductance. In addition, protonation alters the symmetry of the molecular structure, and thus the interfacial potential decreases. In a similar way, the charge transport capabilities can be substantially tuned^{195,196} by incorporating a phosphonium group into metalla-aromatics or protonating azulene derivatives.

Side-group chemistry. Side-group chemistry has also been used¹⁹⁷ to control the conductance behaviour of molecular junctions based on 4,4'-bipyridine. The introduction of bulky alkyl side groups in the phosphoryl-bridged compounds (FIG. 6d) effectively hinders the mechanically triggered conductance switching. The switching behaviour can be reinstated by substituting the bulky alkyl with a phenyl. In addition, bridging the two pyridine rings with Si-based groups can enhance the switching ratio. In relaxed junctions, the molecule is positioned parallel to the electrode axis, and carrier transport is mainly controlled by the LUMO, with a sharp resonance near E_F . Upon junction compression, the molecule leans against the junction to form a geometric structure in which the pyridyl ring co-facially lies down on the electrode. In the bare bipyridine molecular junction, the compressed structure leads to strong interface coupling and high conductance. However, only a small difference in transmission between the relaxed and compressed junctions was observed in molecules II-2 and II-3: a bulky side group induces Au–N stretching, which reduces the electronic coupling with the electrode. As for molecules II-4 and

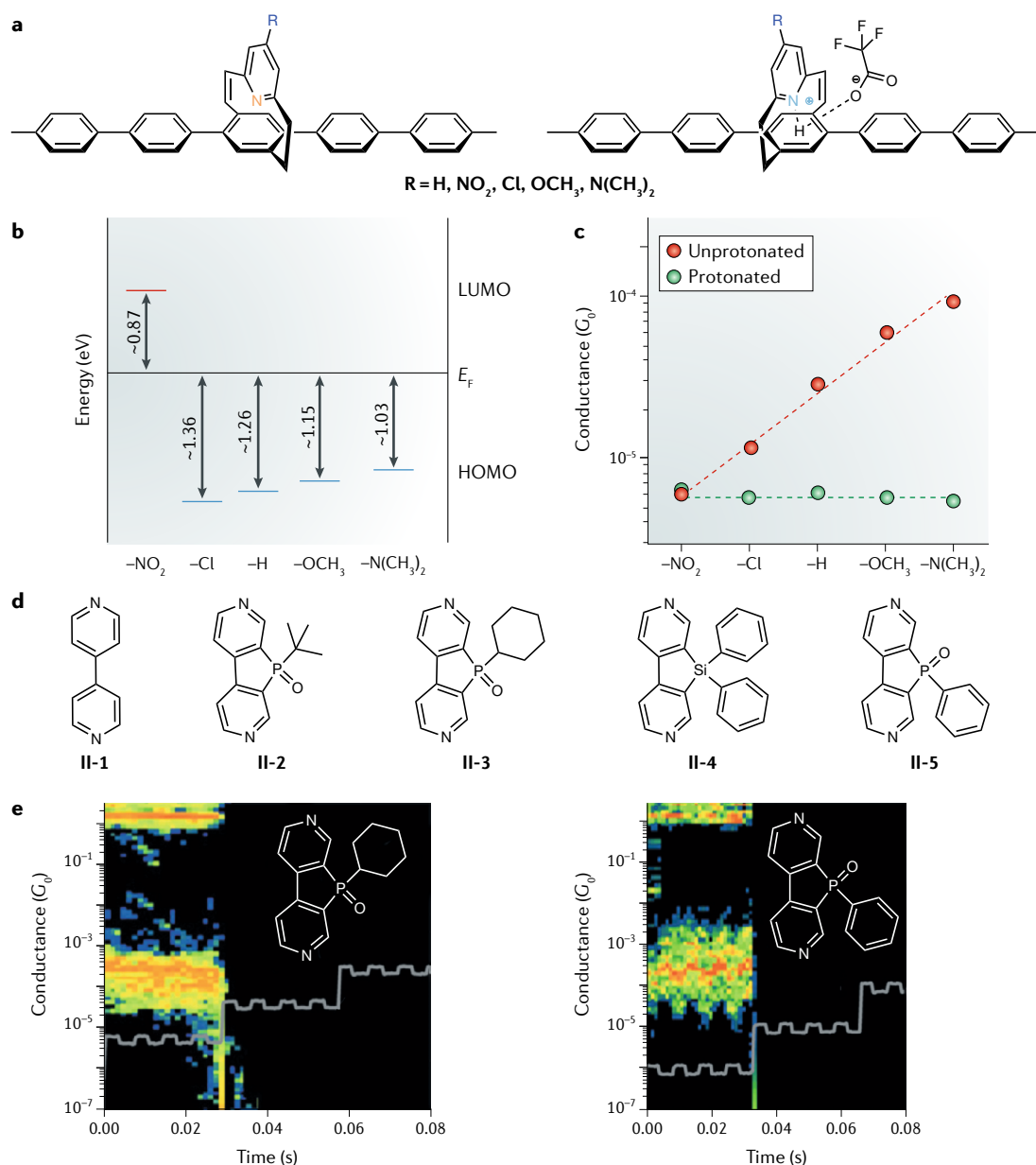


Fig. 6 | Use of substituents to tune the conductance in single-molecule junctions. a | Chemical structures of cyclophanes with different side groups, and the corresponding protonated forms (chemical structures from REF.¹⁹³). **b** | Effect of substituent groups on the energy gaps between the dominant orbital (lowest unoccupied molecular orbital, LUMO, or highest occupied molecular orbital, HOMO) and the Fermi energy (E_F). **c** | Difference between the conductances of the molecules with and without protonation in the cyclophane wires. **d** | Chemical structures of 4,4'-bipyridines with different side groups used to control their conductance (chemical structures from REF.¹⁹⁷). **e** | Piezo-controlled conductance characteristics of II-3 and II-5 show larger conductance in II-5 owing to the interaction between the electrodes and the π -systems of the phenyl side groups. The 2D maps with piezo signals superimposed as grey lines show two distinctive conductance states for II-5 but not for II-3. G_0 , effective constant conductance. Panel **b** is reproduced with permission from REFS¹⁹³, ACS. Panel **c** is adapted with permission from REF.¹⁹⁴, RSC. Panel **e** is adapted with permission from REF.¹⁹⁷, Wiley-VCH.

II-5, although the binding geometric structure at the cofacial end is the same as in molecules II-2 and II-3, strong interactions between the electrodes and the π -systems of the phenyl side groups enhance the coupling, as well as the conductivity (FIG. 6e).

These results prove that it is possible to modulate in situ electronic structure (and thus the conductance) of single-molecule junctions by external stimuli, in this case, the rearrangement of the molecular electronic

structures caused by either intermolecular interaction or chemical reactivity¹⁹⁸. Because the substituent groups are affected in a limited way by interface coupling and their structural or electronic alterations result in minor changes in charge transport in the molecular backbone, the design of more controllable groups in the substituent position will provide more opportunities for the construction of stable molecular devices with specific physical properties. One key consideration to realize

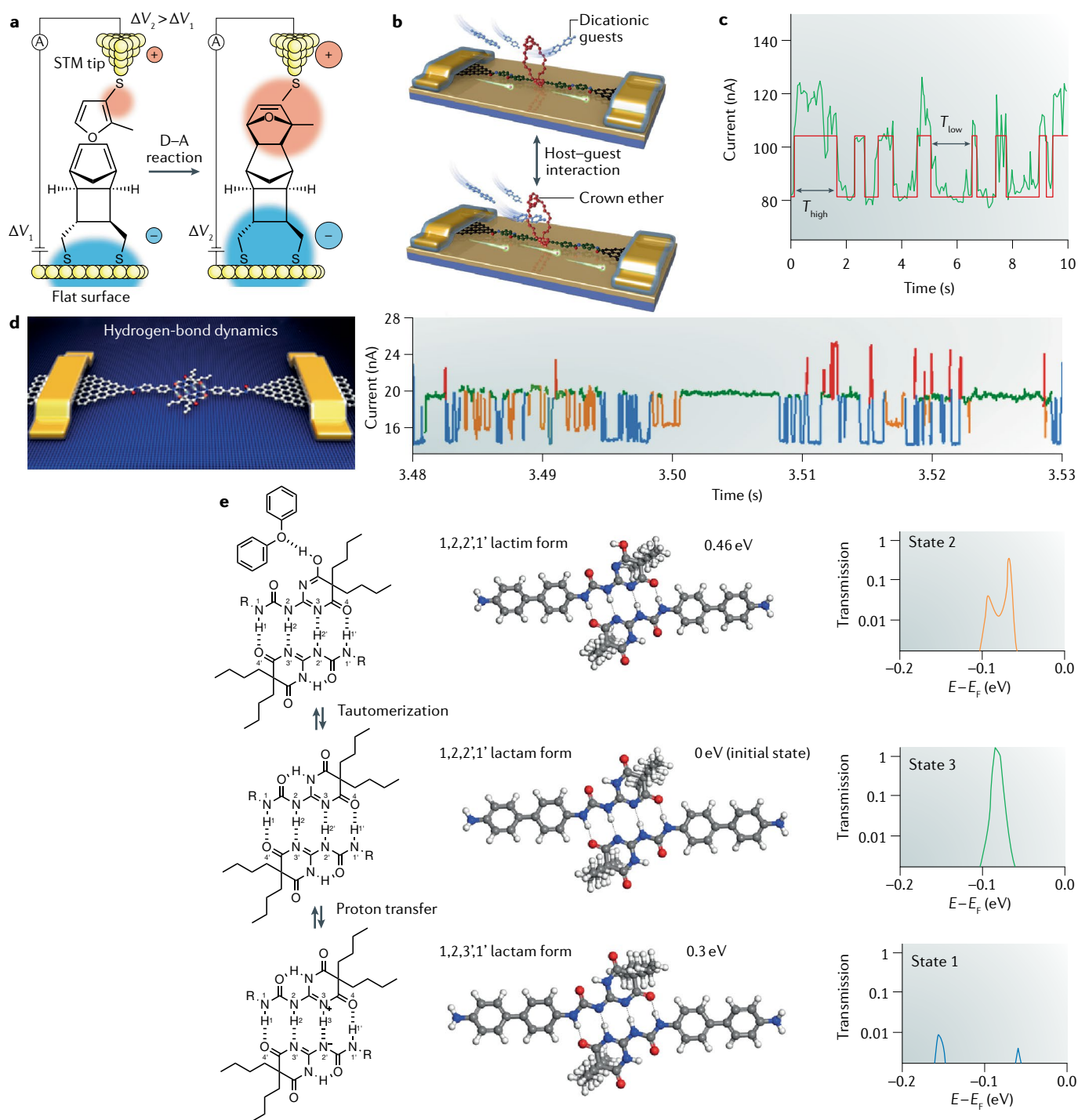


Fig. 7 | Single-molecule dynamic detection of intermolecular reactions or interactions. **a** | Schematic representation of a Diels-Alder (D-A) reaction under the external electric field of a scanning tunnelling microscopy (STM)-based junction. The diene and dienophile were attached to the STM tip and to the flat gold surface through thiol groups. **b** | Schematic representation of the pseudorotaxane formation (right panel) and deformation (left panel) processes that occur when a dicationic guest interacts with the crown ether. **c** | Current-time curve of a pseudorotaxane-based device in a Me_2SO solution containing 1 mM methyl viologen (MV)-2PF₆ (293 K) with the corresponding idealized fit obtained from the segmental *k*-means method based on hidden Markov model analysis. The low and high conductance states were attributed to the deformation and formation states, respectively. The source-drain bias is 100 mV, and the gate bias is 0 mV. **d** | Schematic representation of a single-molecule junction based on a quadrupolar hydrogen-bonded system and current-time curves for a device in diphenyl ether at 323 K. **e** | Schematic diagram of each transformation process (left panels) with the low-lying energy (*E*) structures (middle panels) and corresponding transmission spectra at zero bias voltage (right panels). A, ammeter; E_F , Fermi energy; *T*, temperature; V, voltage. Panel **a** is adapted from REF.²⁰⁴, Springer Nature Limited. Panels **b** and **c** are reproduced with permission from REF.²⁰³, AAAS. Panels **d** and **e** are adapted from REF.²⁰⁶, CC-BY-4.0.

high-quality optoelectronic devices and switches is that the different states of the functional groups should have distinct electronic effects on the backbone. Because the substituent groups are not directly involved in charge transport, this strategy provides an ideal way to investigate the intrinsic effect of external stimuli (for example, the electric field between the electrodes) on the physical behaviour of the molecules without the interference from tunnelling currents. This might also lead to the direct observation of physical phenomena that are not accessible by conventional approaches. More importantly, these behaviours might enable a single-molecule realization of label-free, real-time electrical measurements of fast interaction dynamics with single-event sensitivity^{45,47,199–202}.

Chemical reactions studied by single-molecule junctions. The use of single-molecule junctions to study step-by-step chemical reactions and interactions at the single-event level in a dynamic manner was recently demonstrated^{203–208}. For instance, STM-based break junctions enabled the observation of the Diels–Alder reaction between a furan diene and dienophile initiated by an external electrical field²⁰⁴ (FIG. 7a); the researchers tried to electrostatically stabilize the resonance structure of the transition state using the downward electric field orientation at the negative bias. The photothermal reaction process of a photochromic dihydroazulene–vinylheptafulvene system was studied²⁰⁷ with MCBJs, revealing that the junction environment substantially influences the chemical process. Single-molecule junctions based on graphene⁵¹ were exploited to improve the stability of the device and duration of the measurement. A functional molecular bridge was covalently integrated with an electron-rich crown ether into graphene nanoelectrodes, enabling direct probing of the physical pseudorotaxane formation and deformation processes when a dicationic guest interacts with the crown ether with microsecond resolution (FIG. 7b)²⁰³. This technique can quantify the binding and unbinding rate constants and the activation energies for host–guest interactions (FIG. 7c).

In addition to the characterization of host–guest interactions, this technique was extended to address hydrogen-bond assembly dynamics with single-bond resolution²⁰⁶. A quadrupolar hydrogen-bonding system was covalently immobilized into graphene point contacts to establish a stable supramolecule-assembled single-molecule junction (FIG. 7d). The dynamics of individual hydrogen bonds in different solvents at different temperatures were studied in combination with density functional theory. In diphenyl ether, different current spikes and multiple levels of current signals were observed at 323 K (FIG. 7d), and the spikes and plateaus were classified into four microstates according to their amplitudes. Theoretical calculations for both the energy and transmission spectra at a zero bias voltage suggest that each current stage can be attributed to a different configuration. The transformation process was understood as follows (FIG. 7e): from the initial state (state 3), a 1,2,2',1' lactam form, the hydrogen atom on N2' is reversibly transferred to N3, forming a dissymmetric

tautomer, the 1,2,3,1' lactam form, with low conductivity (state 1); or through lactam–lactim tautomerism, the 1,2,2',1' lactam form is converted into a 1,2,2',1' lactim form that constitutes the intermediate conducting state of state 2. State 4 shows spike-like, high-frequency features. This probably results from the stabilizing effects of diphenyl ether molecules. Therefore, the observed multimodal distribution mainly results from stochastic rearrangements of the hydrogen-bond structure through either intermolecular proton transfer or lactam–lactim tautomerism. This work demonstrates an approach for probing weak bond interaction dynamics at the single-event level.

Beyond supramolecular chemistry, single-molecule electrical detection has potential for revealing temporal and reaction trajectories of individual intermediates in elementary reactions. To this end, a single diarylethene molecule with three methylene groups on each side was designed and synthesized, with the aim of decreasing the strong molecule–electrode coupling³⁵. When covalently sandwiched between graphene electrodes (FIG. 8a), this molecule showed reversible linkage and breakage of a single σ -bond in the diarylethene centre driven by UV and visible light irradiation, thus leading to reversible and stable conductance photoswitching at room temperature (FIG. 8b). However, the attempt to capture the intermediates produced during the process of σ -bond linkage and breakage failed because the reaction is too quick to follow. To this end, most recently, a molecular wire with a 9-fluorenone centre was designed and covalently connected to nano-gapped graphene electrodes to establish functional single-molecule junctions (FIG. 8c)²⁰⁵. In situ electrical measurements at the molecular level demonstrated notable and reproducible current fluctuations with obvious solvent dependence in a nucleophilic addition reaction between hydroxylamine and a carbonyl group (FIG. 8d). In combination with theoretical simulations (FIG. 8e), it was demonstrated that this observation can be attributed to the reversible reaction between the ketone sidearm and an intermediate (FIG. 8d), which happens in a few microseconds. Beyond reaction chemistry, such a nanocircuit-based architecture offers a new strategy for the label-free exploration of rapid single-molecule (bio)physics or for single-molecule detection with high temporal resolution.

Conclusions and perspectives

In this Review, adopting an engineering point of view encompassing three aspects — electrode material, interface and molecular bridge — we have systematically discussed current principles for the development of robust single-molecule electronic devices and for the integration of molecular functionalities into molecular electronic devices. The choice of electrode materials, the control of molecule–electrode interface coupling and the design of functional molecular kernels, working together as an intercorrelated holistic system, play a key role in device performance and stability. Molecule–electrode interface coupling, the strength of which is mainly determined by the nature of the contact (physical contact, π – π stacking or covalent binding), is intimately related to the choice of both electrode

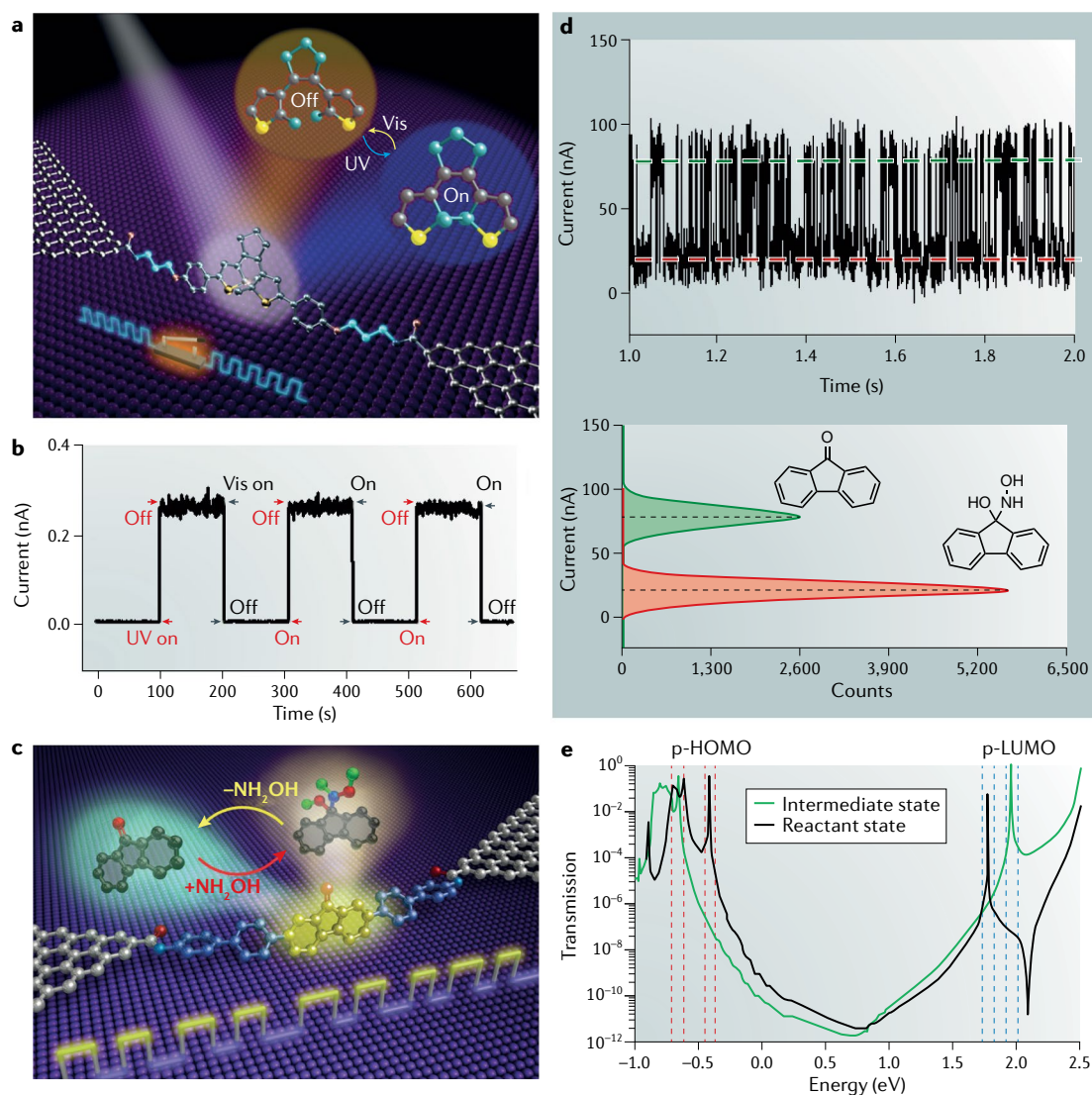


Fig. 8 | Single-molecule dynamic detection of chemical reactions. **a** | Schematic representation of a graphene–diarylethene–graphene single-molecule junction emphasizing the addition of three methylene groups to the molecule and showing the photoswitching mechanism. **b** | Reversible linkage and breakage of a single σ -bond driven by UV and visible (vis) light irradiation leads to reversible and stable conductance photoswitching at room temperature. The source–drain bias is 100 mV, and the gate bias is 0 mV. **c** | Schematic representation of fluorenone-bridged single-molecule junctions that emphasize a nucleophilic addition reaction between hydroxylamine and a carbonyl group. **d** | In situ single-molecule current–time measurements (top panel) in a mixed solution (EtOH:H₂O = 1:4) containing NH₂OH (10 $\mu\text{mol l}^{-1}$) and NaOH (10 $\mu\text{mol l}^{-1}$) at 298 K. The source–drain bias is 300 mV and the gate bias is 0 mV. The corresponding current histogram is presented in the bottom panel, showing a bimodal distribution. **e** | Transmission spectra of the reactant and an intermediate. The red and blue dashed lines highlight the transmission peaks of the perturbed highest occupied molecular orbital (p-HOMO) and perturbed lowest unoccupied molecular orbital (p-LUMO) for both states, whose interactions occur in a few microseconds. Panels **a** and **b** are reproduced with permission from REF.³⁵, AAAS. Panels **c**, **d**, **e** are reproduced with permission from REF.²⁰⁵, AAAS.

materials and anchoring groups. Through the flexible design of molecular bridges (anchoring end group, spacer and functional backbone) and a suitable choice of electrode materials, the molecule–electrode interface can be optimized to precisely control the relative energy gap between the molecular orbital energy levels and the Fermi level of the electrodes, thus contributing to the device stability. This stability is particularly important because it enables testing of different molecular engineering options and makes it possible to carry out reproducible electrical measurements, not only for probing the fundamental properties of materials at the molecular

scale but also for imparting newly designed or even unexpected functionalities (such as switching, rectification, thermoelectricity, QI, sensing and stereoelectronic effects) to electrical nanocircuits. Although molecular electronics is a fairly mature field, tremendous challenges still exist in both scientific research and industrial manufacture.

One of the most critical challenges is the device-to-device uniformity. Once the size of a single electronic device is scaled down to the atomic or molecular level, even variations at the atomic level may influence its conductance performances. Currently, neither metal nor carbon-based electrodes guarantee atomic control

of the electrode geometry, resulting in variant configurations at the molecule–electrode contact interface. For metal leads, the bonding sites for anchoring groups vary from device to device. In addition, the size of metal electrodes is not at the molecular scale. Hence, it is possible that only one molecule links two electrodes, while many others are adsorbed on the electrode surface. This configuration has a notable effect on the charge transport in the molecular bridge; thus, statistical conductivity data acquired from STM-based and MCBJ-based break junctions reveal fluctuations in the device performance. This is detrimental, especially for the functionalization of single-molecule electrical circuits. For carbon-based electrodes, conductance is affected by the edge configuration and inhomogeneous conductance of single-walled carbon nanotubes, even though the edges of the nanotubes and of graphene electrodes are at the atomic scale. The formation of nano-gapped electrodes with atomic-level precision and high yield and the precise control of the contact configuration and molecular conformation within the gaps on the substrate surface are the key issues in the evolution of molecular electronics from laboratory-based research to industrial applications.

Stability is an essential requirement for practical applications of molecular electronics. In single-molecule electronic circuits, molecular junctions, especially those based on metal electrodes, show poor stability. To achieve resonant transport, several volts typically need to be applied to junctions of only a few nanometres, leading to non-equilibrated dynamics and strong coupling between the molecular orbitals and the electric field gradient across the junction. Under such high bias voltages, atoms at both metal and carbon-based electrodes are mobile and tend to diffuse owing to heating effects. Additionally, lone pair species (such as Au–S bonds) are generally used to immobilize the molecules between two metal electrodes, but these coordination bonds are easily oxidized or ruptured. A precise choice of the measurement conditions and the formation of covalent bonds at the electrode–molecule contact interface might be an efficient way to improve device stability.

Another formidable challenge for single-molecule electronics is the integration capability, which is critical for applications. However, it seems that little attention has been paid to this aspect. For STM-based junctions and MCBJs, integration would be difficult owing to the incompatibility with current CMOS-based technologies. Carbon-based molecular junctions are advantageous in this respect owing to their three-terminal device architecture. To date, all reported measurements have been performed in a laboratory environment. However, practical devices are far more complicated and exposed to various operating and interference effects. To achieve

efficient integration, two key factors should be considered. The first is that despite the intrinsically tiny size of their core parts, the long leads and large pads needed for outer connection hinder full exploitation of the potential of molecular devices. The second is that rather than replacing the CMOS technology, molecular devices are likely to be complementary parts within CMOS-based circuits. Hence, molecular devices should be CMOS-compatible to achieve practical applications^{209,210}.

From a theoretical standpoint, the field needs further development. For instance, intrinsic misalignment exists between discrete molecular energy levels and continuous Fermi levels of the electrodes, making it difficult to understand how the voltage drops through the junction. Therefore, theoretical models that can fully explain experimental phenomena at a quantitative level are urgently needed. Moreover, theories should instruct experimental design — of both molecular materials and device architecture — to realize new functionalities. In an ideal scenario, when a specific molecular function is desired, it could be easily realized thanks to a good knowledge of the properties of molecules and of the synthetic routes that would realize the target structure.

The ultimate goal of microelectronics miniaturization is to manipulate the building blocks of matter with atomic-level precision. Only small molecules can offer such accurate control at subnanometre length scales and with the possibility of reproducibly fabricating exactly the same building blocks. Single-molecule electronics might be the only choice for moving beyond Si-based microelectronics. Consequently, there is strong motivation for the development of practical single-molecule optoelectronic devices. Apart from their small dimensions, such devices would also offer brand new functions beyond those achievable with traditional solid-state electrical devices, enabling new applications. Another research area that will profit from a deep understanding of the fundamental properties of materials at the single-molecule level is that of analytical chemistry, whose final goal is single-molecule detection. New modes of characterization might set up a mainstream methodology that enables single-molecule electrical detection for the investigation of single-molecule and single-event dynamics in an interdisciplinary setting. Considering the nature of this interdisciplinary field, only truly strong collaboration among materials scientists, engineers, physicists, electronic engineers, chemists and biologists will advance this powerful technology and foster its rapid development towards applications. Indeed, we trust that single-molecule electronics has a bright future for integrating the organic molecular world with hard electronics.

Published online 25 February 2019

1. Waldrop, M. M. The chips are down for Moore's law. *Nature* **530**, 144–147 (2016).
2. Semiconductor Industry Association. *2015 International Technology Roadmap for Semiconductors (ITRS)* (Semiconductor Industry Association, 2015).
3. Aviram, A. & Ratner, M. A. Molecular rectifiers. *Chem. Phys. Lett.* **29**, 277–283 (1974).
4. Xiang, D., Wang, X., Jia, C., Lee, T. & Guo, X. Molecular-scale electronics: from concept to function. *Chem. Rev.* **116**, 4318–4440 (2016).
5. Metzger, R. M. Unimolecular electronics. *Chem. Rev.* **115**, 5056–5115 (2015).
6. Su, T. A., Neupane, M., Steigerwald, M. L., Venkataraman, L. & Nuckolls, C. Chemical principles of single-molecule electronics. *Nat. Rev. Mater.* **1**, 16002 (2016).
7. Sun, L. et al. Single-molecule electronics: from chemical design to functional devices. *Chem. Soc. Rev.* **43**, 7378–7411 (2014).
8. Amdursky, N. et al. Electronic transport via proteins. *Adv. Mater.* **26**, 7142–7161 (2014).
9. Vilan, A., Aswal, D. & Cahen, D. Large-area, ensemble molecular electronics: motivation and challenges. *Chem. Rev.* **117**, 4248–4286 (2017).
10. Li, T., Hu, W. & Zhu, D. Nanogap electrodes. *Adv. Mater.* **22**, 286–300 (2010).
11. Reed, M. A., Zhou, C., Muller, C. J., Burgin, T. P. & Tour, J. M. Conductance of a molecular junction. *Science* **278**, 252–254 (1997).
12. Xiang, D., Jeong, H., Lee, T. & Mayer, D. Mechanically controllable break junctions for molecular electronics. *Adv. Mater.* **25**, 4845–4867 (2013).

13. Huang, C., Rudnev, A. V., Hong, W. & Wandlowski, T. Break junction under electrochemical gating: testbed for single-molecule electronics. *Chem. Soc. Rev.* **44**, 889–901 (2015).
14. Cui, X. D. et al. Reproducible measurement of single-molecule conductivity. *Science* **294**, 571–574 (2001).
15. Ho Choi, S., Kim, B. & Frisbie, C. D. Electrical resistance of long conjugated molecular wires. *Science* **320**, 1482–1486 (2008).
16. Park, J. et al. Coulomb blockade and the Kondo effect in single-atom transistors. *Nature* **417**, 722–725 (2002).
17. Liang, W., Shores, M. P., Bockrath, M., Long, J. R. & Park, H. Kondo resonance in a single-molecule transistor. *Nature* **417**, 725–729 (2002).
18. Xu, B. & Tao, N. J. Measurement of single-molecule resistance by repeated formation of molecular junctions. *Science* **301**, 1221–1223 (2003).
19. Venkataraman, L., Klare, J. E., Nuckolls, C., Hybertsen, M. S. & Steigerwald, M. L. Dependence of single-molecule junction conductance on molecular conformation. *Nature* **442**, 904–907 (2006).
20. Qin, L., Park, S., Huang, L. & Mirkin, C. A. On-wire lithography. *Science* **309**, 113–115 (2005).
21. Guo, X. et al. Covalently bridging gaps in single-walled carbon nanotubes with conducting molecules. *Science* **311**, 356–359 (2006).
22. Cao, Y. et al. Building high-throughput molecular junctions using indented graphene point contacts. *Angew. Chem. Int. Ed.* **51**, 12228–12232 (2012).
23. Tang, J. et al. Encoding molecular-wire formation within nanoscale sockets. *Angew. Chem. Int. Ed.* **119**, 3966–3969 (2007).
24. Kubatkin, S. et al. Single-electron transistor of a single organic molecule with access to several redox states. *Nature* **425**, 698–701 (2003).
25. Rampi, M. A., Schueller, O. J. A. & Whitesides, G. M. Alkanethiol self-assembled monolayers as the dielectric of capacitors with nanoscale thickness. *Appl. Phys. Lett.* **72**, 1781–1783 (1998).
26. Rampi, M. A. & Whitesides, G. M. A versatile experimental approach for understanding electron transport through organic materials. *Chem. Phys.* **281**, 373–391 (2002).
27. Akkerman, H. B., Blom, P. W., de Leeuw, D. M. & de Boer, B. Towards molecular electronics with large-area molecular junctions. *Nature* **441**, 69–72 (2006).
28. Tao, N. J. Electron transport in molecular junctions. *Nat. Nanotechnol.* **1**, 173–181 (2006).
29. Aradhya, S. V. & Venkataraman, L. Single-molecule junctions beyond electronic transport. *Nat. Nanotechnol.* **8**, 399–410 (2013).
30. Moth-Poulsen, K. & Bjornholm, T. Molecular electronics with single molecules in solid-state devices. *Nat. Nanotechnol.* **4**, 551–556 (2009).
31. Lindsay, S. M. & Ratner, M. A. Molecular transport junctions: clearing myths. *Adv. Mater.* **19**, 23–31 (2007).
32. Lambert, C. J. Basic concepts of quantum interference and electron transport in single-molecule electronics. *Chem. Soc. Rev.* **44**, 875–888 (2015).
33. Guedon, C. M. et al. Observation of quantum interference in molecular charge transport. *Nat. Nanotechnol.* **7**, 305–309 (2012).
34. Ballmann, S. et al. Experimental evidence for quantum interference and vibrationally induced decoherence in single-molecule junctions. *Phys. Rev. Lett.* **109**, 056801 (2012).
35. Jia, C. et al. Covalently bonded single-molecule junctions with stable and reversible photoswitched conductivity. *Science* **352**, 1443–1445 (2016).
36. Liu, Z., Ren, S. & Guo, X. Switching effects in molecular electronic devices. *Top. Curr. Chem.* **375**, 56 (2017).
37. Collier, C. P. A [2]Catenane-based solid state electronically reconfigurable switch. *Science* **289**, 1172–1175 (2000).
38. Zhang, J. L. et al. Towards single molecule switches. *Chem. Soc. Rev.* **44**, 2998–3022 (2015).
39. Reddy, P., Jang, S. Y., Segalman, R. A. & Majumdar, A. Thermoelectricity in molecular junctions. *Science* **315**, 1568–1571 (2007).
40. Nozaki, D., Avdoshenko, S. M., Sevincli, H. & Cuniberti, G. Quantum interference in thermoelectric molecular junctions: a toy model perspective. *J. Appl. Phys.* **116**, 074308 (2014).
41. Elbing, M. et al. A single-molecule diode. *Proc. Natl Acad. Sci. USA* **102**, 8815–8820 (2005).
42. Kim, W. Y. & Kim, K. S. Tuning molecular orbitals in molecular electronics and spintronics. *Acc. Chem. Res.* **43**, 111–120 (2010).
43. Sanvito, S. Molecular spintronics. *Chem. Soc. Rev.* **40**, 3336–3355 (2011).
44. Guo, X. Single-molecule electrical biosensors based on single-walled carbon nanotubes. *Adv. Mater.* **25**, 3397–3408 (2013).
45. Zhao, Y. et al. Single-molecule spectroscopy of amino acids and peptides by recognition tunnelling. *Nat. Nanotechnol.* **9**, 466–473 (2014).
46. Wang, J. et al. Point decoration of silicon nanowires: an approach toward single-molecule electrical detection. *Angew. Chem. Int. Ed.* **53**, 5038–5043 (2014).
47. He, G., Li, J., Ci, H., Qi, C. & Guo, X. Direct measurement of single-molecule DNA hybridization dynamics with single-base resolution. *Angew. Chem. Int. Ed.* **55**, 9036–9040 (2016).
48. Zhang, J. et al. Single-molecule electron transfer in electrochemical environments. *Chem. Rev.* **108**, 2737–2791 (2008).
49. Shen, Q., Guo, X., Steigerwald, M. L. & Nuckolls, C. Integrating reaction chemistry into molecular electronic devices. *Chemistry Asian J.* **5**, 1040–1057 (2010).
50. Perrin, M. L., Burzuri, E. & van der Zant, H. S. Single-molecule transistors. *Chem. Soc. Rev.* **44**, 902–919 (2015).
51. Jia, C., Ma, B., Xin, N. & Guo, X. Carbon electrode-molecule junctions: a reliable platform for molecular electronics. *Acc. Chem. Res.* **48**, 2565–2575 (2015).
52. Su, T. A. et al. Silane and germane molecular electronics. *Acc. Chem. Res.* **50**, 1088–1095 (2017).
53. Cuevas, J. C. & Scheer, E. *Molecular Electronics: An Introduction to Theory and Experiment* Vol. 15 (World Scientific, 2017).
54. Landauer, R. Spatial variation of currents and fields due to localized scatterers in metallic conduction. *IBM J. Res. Dev.* **1**, 223–231 (1957).
55. Büttiker, M., Imry, Y., Landauer, R. & Pinhas, S. Generalized many-channel conductance formula with application to small rings. *Phys. Rev. B* **31**, 6207–6215 (1985).
56. Eränen, S. & Sinkkonen, J. Generalization of the Landauer conductance formula. *Phys. Rev. B* **35**, 2222–2227 (1987).
57. Nitzan, A. Electron transmission through molecules and molecular interfaces. *Annu. Rev. Phys. Chem.* **52**, 681–750 (2001).
58. Xue, Y. & Ratner, M. A. Microscopic study of electrical transport through individual molecules with metallic contacts. II. Effect of the interface structure. *Phys. Rev. B* **68**, 115407 (2003).
59. Yelin, T. et al. Conductance saturation in a series of highly transmitting molecular junctions. *Nat. Mater.* **15**, 444–449 (2016).
60. Jia, C. et al. Conductance switching and mechanisms in single-molecule junctions. *Angew. Chem. Int. Ed.* **52**, 8666–8670 (2013).
61. Dulic, D. et al. One-way optoelectronic switching of photochromic molecules on gold. *Phys. Rev. Lett.* **91**, 207402 (2003).
62. Whalley, A. C., Steigerwald, M. L., Guo, X. & Nuckolls, C. Reversible switching in molecular electronic devices. *J. Am. Chem. Soc.* **129**, 12590–12591 (2007).
63. Frisbie, C. D. Designing a robust single-molecule switch. *Science* **352**, 1394–1395 (2016).
64. Jia, C. & Guo, X. Molecule-electrode interfaces in molecular electronic devices. *Chem. Soc. Rev.* **42**, 5642–5660 (2013).
65. Bruot, C., Hihath, J. & Tao, N. Mechanically controlled molecular orbital alignment in single molecule junctions. *Nat. Nanotechnol.* **7**, 35–40 (2011).
66. Kim, T. et al. Determination of energy level alignment and coupling strength in 4,4'-bipyridine single-molecule junctions. *Nano Lett.* **14**, 794–798 (2014).
67. Thygesen, K. S. & Rubio, A. Renormalization of molecular quasiparticle levels at metal-molecule interfaces: trends across binding regimes. *Phys. Rev. Lett.* **102**, 046802 (2009).
68. Perrin, M. L. et al. Large tunable image-charge effects in single-molecule junctions. *Nat. Nanotechnol.* **8**, 282–287 (2013).
69. Kaasbjerg, K. & Flensberg, K. Strong polarization-induced reduction of addition energies in single-molecule nanojunctions. *Nano Lett.* **8**, 3809–3814 (2008).
70. Park, Y. S. et al. Contact chemistry and single-molecule conductance: a comparison of phosphines, methyl sulfides, and amines. *J. Am. Chem. Soc.* **129**, 15768–15769 (2007).
71. Arroyo, C. R. et al. Influence of binding groups on molecular junction formation. *J. Am. Chem. Soc.* **133**, 14313–14319 (2011).
72. Li, H. et al. Electric field breakdown in single molecule junctions. *J. Am. Chem. Soc.* **137**, 5028–5033 (2015).
73. Moreno-García, P. et al. Single-molecule conductance of functionalized oligynes: length dependence and junction evolution. *J. Am. Chem. Soc.* **135**, 12228–12240 (2013).
74. Tsutsui, M., Taniguchi, M. & Kawai, T. Quantitative evaluation of metal-molecule contact stability at the single-molecule level. *J. Am. Chem. Soc.* **131**, 10552–10556 (2009).
75. Hong, W. et al. Single molecular conductance of tolans: experimental and theoretical study on the junction evolution dependent on the anchoring group. *J. Am. Chem. Soc.* **134**, 2292–2304 (2012).
76. Schwarz, F. et al. High-conductive organometallic molecular wires with delocalized electron systems strongly coupled to metal electrodes. *Nano Lett.* **14**, 5932–5940 (2014).
77. Ponce, J. et al. Effect of metal complexation on the conductance of single-molecule wires measured at room temperature. *J. Am. Chem. Soc.* **136**, 8314–8322 (2014).
78. Hong, W. et al. Trimethylsilyl-terminated oligo(phenylene ethynylene)s: an approach to single-molecule junctions with covalent Au–C sigma-bonds. *J. Am. Chem. Soc.* **134**, 19425–19431 (2012).
79. Lissel, F. et al. Organometallic single-molecule electronics: tuning electron transport through X(diphosphine)2FeC4Fe(diphosphine)2X building blocks by varying the Fe–X–Au anchoring scheme from coordinative to covalent. *J. Am. Chem. Soc.* **136**, 14560–14569 (2014).
80. Martin, C. A. et al. Fullerene-based anchoring groups for molecular electronics. *J. Am. Chem. Soc.* **130**, 13198–13199 (2008).
81. Leary, E. et al. Unambiguous one-molecule conductance measurements under ambient conditions. *Nano Lett.* **11**, 2236–2241 (2011).
82. Meisner, J. S. et al. Importance of direct metal-pi coupling in electronic transport through conjugated single-molecule junctions. *J. Am. Chem. Soc.* **134**, 20440–20445 (2012).
83. Kiguchi, M. et al. Single molecular resistive switch obtained via sliding multiple anchoring points and varying effective wire length. *J. Am. Chem. Soc.* **136**, 7327–7332 (2014).
84. Quek, S. Y. et al. Mechanically controlled binary conductance switching of a single-molecule junction. *Nat. Nanotechnol.* **4**, 230–234 (2009).
85. Kamenetska, M. et al. Conductance and geometry of pyridine-linked single-molecule junctions. *J. Am. Chem. Soc.* **132**, 6817–6821 (2010).
86. Venkataraman, L. et al. Single-molecule circuits with well-defined molecular conductance. *Nano Lett.* **6**, 458–462 (2006).
87. Quek, S. Y. et al. Amine-gold linked single-molecule circuits: experiment and theory. *Nano Lett.* **7**, 3477–3482 (2007).
88. Rascon-Ramos, H., Artes, J. M., Li, Y. & Hihath, J. Binding configurations and intramolecular strain in single-molecule devices. *Nat. Mater.* **14**, 517–522 (2015).
89. Mishchenko, A. et al. Single-molecule junctions based on nitrile-terminated biphenyls: a promising new anchoring group. *J. Am. Chem. Soc.* **133**, 184–187 (2011).
90. Frei, M., Aradhya, S. V., Hybertsen, M. S. & Venkataraman, L. Linker dependent bond rupture force measurements in single-molecule junctions. *J. Am. Chem. Soc.* **134**, 4003–4006 (2012).
91. Ie, Y. et al. Nature of electron transport by pyridine-based tripodal anchors: potential for robust and conductive single-molecule junctions with gold electrodes. *J. Am. Chem. Soc.* **133**, 3014–3022 (2011).
92. Kim, N. T., Li, H., Venkataraman, L. & Leighton, J. L. High-conductance pathways in ring-strained disilanes by way of direct sigma-Si-Si to Au coordination. *J. Am. Chem. Soc.* **138**, 11505–11508 (2016).
93. Gerhard, L. et al. An electrically actuated molecular toggle switch. *Nat. Commun.* **8**, 14672 (2017).
94. Li, Z. et al. Regulating a benzodifuran single molecule redox switch via electrochemical gating and optimization of molecule/electrode coupling. *J. Am. Chem. Soc.* **136**, 8867–8870 (2014).
95. Xing, Y. et al. Optimizing single-molecule conductivity of conjugated organic oligomers with carbodithioate linkers. *J. Am. Chem. Soc.* **132**, 7946–7956 (2010).
96. von Wrochem, F. et al. Efficient electronic coupling and improved stability with dithiocarbamate-based

- molecular junctions. *Nat. Nanotechnol.* **5**, 618–624 (2010).
97. Hong, Z. –W. et al. Quantum interference effect of single–molecule conductance influenced by insertion of different alkyl length. *Electrochem. Commun.* **68**, 86–89 (2016).
 98. Bagrets, A., Arnold, A. & Evers, F. Conduction properties of bipyridinium–functionalized molecular wires. *J. Am. Chem. Soc.* **130**, 9013–9018 (2008).
 99. Adak, O., Korytar, R., Joe, A. Y., Evers, F. & Venkataraman, L. Impact of electrode density of states on transport through pyridine–linked single–molecule junctions. *Nano Lett.* **15**, 3716–3722 (2015).
 100. Li, H. et al. Silver makes better electrical contacts to thiol–terminated silanes than gold. *Angew. Chem. Int. Ed.* **56**, 14145–14148 (2017).
 101. Ko, C. H., Huang, M. J., Fu, M. D. & Chen, C. H. Superior contact for single–molecule conductance: electronic coupling of thiolate and isothiocyanate on Pt, Pd, and Au. *J. Am. Chem. Soc.* **132**, 756–764 (2010).
 102. Bonifas, A. P. & McCreery, R. L. ‘Soft’ Au, Pt and Cu contacts for molecular junctions through surface–diffusion–mediated deposition. *Nat. Nanotechnol.* **5**, 612–617 (2010).
 103. Li, Y. et al. Atomic and electronic structures of a single oxygen molecular junction with Au, Ag, and Cu electrodes. *J. Phys. Chem. C* **120**, 16254–16258 (2016).
 104. Li, Y., Kaneko, S., Fujii, S. & Kiguchi, M. Symmetry of single hydrogen molecular junction with Au, Ag, and Cu electrodes. *J. Phys. Chem. C* **119**, 19143–19148 (2015).
 105. Yoshida, K. et al. Gate–tunable large negative tunnel magnetoresistance in Ni–C60–Ni single molecule transistors. *Nano Lett.* **13**, 481–485 (2013).
 106. Rakhmievitch, D., Sarkar, S., Bitton, O., Kronik, L. & Tal, O. Enhanced magnetoresistance in molecular junctions by geometrical optimization of spin–selective orbital hybridization. *Nano Lett.* **16**, 1741–1745 (2016).
 107. Brooke, R. J. et al. Single–molecule electrochemical transistor utilizing a nickel–pyridyl spinterface. *Nano Lett.* **15**, 275–280 (2015).
 108. Li, J. J. et al. Giant single–molecule anisotropic magnetoresistance at room temperature. *J. Am. Chem. Soc.* **137**, 5923–5929 (2015).
 109. Scott, G. D. & Hu, T. C. Gate–controlled Kondo effect in a single–molecule transistor with elliptical ferromagnetic leads. *Phys. Rev. B* **96**, 144416 (2017).
 110. Lortscher, E. Wiring molecules into circuits. *Nat. Nanotechnol.* **8**, 381–384 (2013).
 111. Prins, F. et al. Room–temperature gating of molecular junctions using few–layer graphene nanogap electrodes. *Nano Lett.* **11**, 4607–4611 (2011).
 112. Xu, Q. et al. Single electron transistor with single aromatic ring molecule covalently connected to graphene nanogaps. *Nano Lett.* **17**, 5335–5341 (2017).
 113. Mol, J. A. et al. Graphene–porphyrin single–molecule transistors. *Nanoscale* **7**, 13181–13185 (2015).
 114. Cao, Y., Dong, S., Liu, S., Liu, Z. & Guo, X. Toward functional molecular devices based on graphene–molecule junctions. *Angew. Chem. Int. Ed.* **52**, 3906–3910 (2013).
 115. Aragones, A. C. et al. Single–molecule electrical contacts on silicon electrodes under ambient conditions. *Nat. Commun.* **8**, 15056 (2017).
 116. Vezzoli, A. et al. Single–molecule transport at a rectifying GaAs contact. *Nano Lett.* **17**, 1109–1115 (2017).
 117. Vezzoli, A., Brooke, R. J., Higgins, S. J., Schwarzacher, W. & Nichols, R. J. Single–molecule photocurrent at a metal–molecule–semiconductor junction. *Nano Lett.* **17**, 6702–6707 (2017).
 118. Capozzi, B. et al. Single–molecule diodes with high rectification ratios through environmental control. *Nat. Nanotechnol.* **10**, 522–527 (2015).
 119. Kim, T., Liu, Z. F., Lee, C., Neaton, J. B. & Venkataraman, L. Charge transport and rectification in molecular junctions formed with carbon–based electrodes. *Proc. Natl Acad. Sci. USA* **111**, 10928–10932 (2014).
 120. Zhang, Q. et al. Graphene as a promising electrode for low–current attenuation in nonsymmetric molecular junctions. *Nano Lett.* **16**, 6534–6540 (2016).
 121. Warner, B. et al. Tunable magnetoresistance in an asymmetrically coupled single–molecule junction. *Nat. Nanotechnol.* **10**, 259–263 (2015).
 122. Bagrets, A. et al. Single molecule magnetoresistance with combined antiferromagnetic and ferromagnetic electrodes. *Nano Lett.* **12**, 5131–5136 (2012).
 123. Derosa, P. A., Guda, S. & Seminario, J. M. A programmable molecular diode driven by charge–induced conformational changes. *J. Am. Chem. Soc.* **125**, 14240–14241 (2003).
 124. Batra, A. et al. Tuning rectification in single–molecular diodes. *Nano Lett.* **13**, 6233–6237 (2013).
 125. Zhang, N., Lo, W. Y., Cai, Z., Li, L. & Yu, L. Molecular rectification tuned by through–space gating effect. *Nano Lett.* **17**, 308–312 (2017).
 126. Perrin, M. L. et al. Single–molecule resonant tunneling diode. *J. Phys. Chem. C* **119**, 5697–5702 (2015).
 127. Diez–Pérez, I. et al. Rectification and stability of a single molecular diode with controlled orientation. *Nat. Chem.* **1**, 635–641 (2009).
 128. Lörtscher, E. et al. Transport properties of a single–molecule diode. *ACS Nano* **6**, 4931–4939 (2012).
 129. McConnell, H. M. Intra-molecular charge transfer in aromatic free radicals. *J. Chem. Phys.* **35**, 508–515 (1961).
 130. Segal, D. & Nitzan, A. Theoretical study of long–range electron transport in molecular junctions. *J. Phys. Chem. B* **104**, 3817–3829 (2000).
 131. Berlin, Y. A., Hutchison, G. R., Rempala, P., Ratner, M. A. & Michel, J. Charge hopping in molecular wires as a sequence of electron–transfer reactions. *J. Phys. Chem. A* **107**, 3970–3980 (2003).
 132. Park, Y. S. et al. Interface–contact chemistry and single–molecule conductance: a comparison of phosphines, methyl sulfides, and amines. *J. Am. Chem. Soc.* **129**, 15768–15768 (2007).
 133. Xing, Y. et al. Optimizing single–molecule conductivity of conjugated organic oligomers with carbodithioate linkers. *J. Am. Chem. Soc.* **132**, 7946–7956 (2010).
 134. Luo, L. et al. Length and temperature dependent conduction of ruthenium–containing redox–active molecular wires. *J. Phys. Chem. C* **115**, 19955–19961 (2011).
 135. Milan, D. C. et al. Solvent dependence of the single molecule conductance of oligoyn–based molecular wires. *J. Phys. Chem. C* **120**, 15666–15674 (2015).
 136. Malen, J. A. et al. Identifying the length dependence of orbital alignment and contact coupling in molecular heterojunctions. *Nano Lett.* **9**, 1164–1169 (2009).
 137. He, J. et al. Electronic decay constant of carotenoid polyenes from single–molecule measurements. *J. Am. Chem. Soc.* **127**, 1384–1385 (2005).
 138. Widawsky, J. R. et al. Length–dependent thermopower of highly conducting Au–C bonded single molecule junctions. *Nano Lett.* **13**, 2889–2894 (2013).
 139. Tan, A. et al. Effect of length and contact chemistry on the electronic structure and thermoelectric properties of molecular junctions. *J. Am. Chem. Soc.* **133**, 8838–8841 (2011).
 140. Capozzi, B. et al. Length–dependent conductance of oligothiophenes. *J. Am. Chem. Soc.* **136**, 10486–10492 (2014).
 141. Yamada, R., Kumazawa, H., Noutoshi, T., Tanaka, S. & Tada, H. Electrical conductance of oligothiophene molecular wires. *Nano Lett.* **8**, 1237–1240 (2008).
 142. Dell, E. J., Capozzi, B., Xia, J., Venkataraman, L. & Campos, L. M. Molecular length dictates the nature of charge carriers in single–molecule junctions of oxidized oligothiophenes. *Nat. Chem.* **7**, 209–214 (2015).
 143. Li, Z., Park, T. H., Rawson, J., Therien, M. J. & Borguet, E. Quasi–ohmic single molecule charge transport through highly conjugated meso–to–meso ethyne–bridged porphyrin wires. *Nano Lett.* **12**, 2722–2727 (2012).
 144. Sedghi, G. et al. Long–range electron tunnelling in oligo–porphyrin molecular wires. *Nat. Nanotechnol.* **6**, 517–523 (2011).
 145. Hines, T. et al. Transition from tunneling to hopping in single molecular junctions by measuring length and temperature dependence. *J. Am. Chem. Soc.* **132**, 11658–11664 (2010).
 146. Cai, Z. et al. Exceptional single–molecule transport properties of ladder–type heteroacene molecular wires. *J. Am. Chem. Soc.* **138**, 10630–10635 (2016).
 147. Lu, Q. et al. From tunneling to hopping: a comprehensive investigation of charge transport mechanism in molecular junctions based on oligo(p–phenylene ethynylene)s. *ACS Nano* **3**, 3861–3868 (2009).
 148. Ashraf, M. K., Bruque, N. A., Tan, J. L., Beran, G. J. & Lake, R. K. Conductance switching in diarylethenes bridging carbon nanotubes. *J. Chem. Phys.* **134**, 024524 (2011).
 149. van der Molen, S. J. et al. Light–controlled conductance switching of ordered metal–molecule–metal devices. *Nano Lett.* **9**, 76–80 (2009).
 150. Irie, M. Diarylethenes for memories and switches. *Chem. Rev.* **100**, 1685–1716 (2000).
 151. Tam, E. S. et al. Single–molecule conductance of pyridine–terminated dithienylethene switch molecules. *ACS Nano* **5**, 5115–5123 (2011).
 152. Kim, Y. et al. Charge transport characteristics of diarylethene photoswitching single–molecule junctions. *Nano Lett.* **12**, 3736–3742 (2012).
 153. Roldan, D. et al. Charge transport in photoswitchable dimethyldihydroxyprylene–type single–molecule junctions. *J. Am. Chem. Soc.* **135**, 5974–5977 (2013).
 154. Haiss, W. et al. Redox state dependence of single molecule conductivity. *J. Am. Chem. Soc.* **125**, 15294–15295 (2003).
 155. Tsoi, S. et al. Electrochemically controlled conductance switching in a single molecule: quinone–modified oligo(phenylene vinylene). *ACS Nano* **2**, 1289–1295 (2008).
 156. Pobelov, I. V., Li, Z. H. & Wandlowski, T. Electrolyte gating in redox–active tunneling junctions—an electrochemical STM approach. *J. Am. Chem. Soc.* **130**, 16045–16054 (2008).
 157. Chen, F. et al. A molecular switch based on potential–induced changes of oxidation state. *Nano Lett.* **5**, 503–506 (2005).
 158. Li, C. et al. Electrochemical gate–controlled electron transport of redox–active single perylene bisimide molecular junctions. *J. Phys. Condens. Matter* **20**, 374122 (2008).
 159. Darwish, N. et al. Observation of electrochemically controlled quantum interference in a single anthraquinone–based norbornylogous bridge molecule. *Angew. Chem. Int. Ed.* **51**, 3203–3206 (2012).
 160. Albrecht, T., Guckian, A., Kuznetsov, A. M., Vos, J. G. & Ulstrup, J. Mechanism of electrochemical charge transport in individual transition metal complexes. *J. Am. Chem. Soc.* **128**, 17132–17138 (2006).
 161. Zhou, X. S. et al. Do molecular conductances correlate with electrochemical rate constants? Experimental insights. *J. Am. Chem. Soc.* **133**, 7509–7516 (2011).
 162. Xiao, X. et al. Redox–gated electron transport in electrically wired ferrocene molecules. *Chem. Phys.* **326**, 138–143 (2006).
 163. Ricci, A. M., Calvo, E. J., Martin, S. & Nichols, R. J. Electrochemical scanning tunneling spectroscopy of redox–active molecules bound by Au–C bonds. *J. Am. Chem. Soc.* **132**, 2494–2495 (2010).
 164. Ting, T. C. et al. Energy–level alignment for single–molecule conductance of extended metal–atom chains. *Angew. Chem. Int. Ed.* **54**, 15734–15738 (2015).
 165. Green, J. E. et al. A 160–kilobit molecular electronic memory patterned at 10¹¹ bits per square centimetre. *Nature* **445**, 414–417 (2007).
 166. Li, Y. et al. Three–state single–molecule naphthalenediimide switch: integration of a pendant redox unit for conductance tuning. *Angew. Chem. Int. Ed.* **54**, 13586–13589 (2015).
 167. Liu, J. et al. Radical–enhanced charge transport in single–molecule phenothiazine electrical junctions. *Angew. Chem. Int. Ed.* **56**, 13061–13065 (2017).
 168. Yin, X. et al. A reversible single–molecule switch based on activated antiaromaticity. *Sci. Adv.* **3**, ea02615 (2017).
 169. Bousseksou, A., Molnar, G., Salmon, L. & Nicolazzi, W. Molecular spin crossover phenomenon: recent achievements and prospects. *Chem. Soc. Rev.* **40**, 3313–3335 (2011).
 170. Thiele, S. et al. Electrically driven nuclear spin resonance in single–molecule magnets. *Science* **344**, 1135–1138 (2014).
 171. Natterer, F. D. et al. Reading and writing single–atom magnets. *Nature* **543**, 226–228 (2017).
 172. Harzmann, G. D., Frisenda, R., van der Zant, H. S. & Mayor, M. Single–molecule spin switch based on voltage–triggered distortion of the coordination sphere. *Angew. Chem. Int. Ed.* **54**, 13425–13430 (2015).
 173. Schwarz, F. et al. Field–induced conductance switching by charge–state alternation in organometallic single–molecule junctions. *Nat. Nanotechnol.* **11**, 170–176 (2016).
 174. Frisenda, R., Janssen, V. A., Grozema, F. C., van der Zant, H. S. & Renaud, N. Mechanically controlled quantum interference in individual pi–stacked dimers. *Nat. Chem.* **8**, 1099–1104 (2016).

175. Manrique, D. Z. et al. A quantum circuit rule for interference effects in single-molecule electrical junctions. *Nat. Commun.* **6**, 6389 (2015).
176. Solomon, G. C., Herrmann, C., Hansen, T., Mujica, V. & Ratner, M. A. Exploring local currents in molecular junctions. *Nat. Chem.* **2**, 223–228 (2010).
177. Vazquez, H. et al. Probing the conductance superposition law in single-molecule circuits with parallel paths. *Nat. Nanotechnol.* **7**, 663–667 (2012).
178. Rabache, V. et al. Direct observation of large quantum interference effect in anthraquinone solid-state junctions. *J. Am. Chem. Soc.* **135**, 10218–10221 (2013).
179. Markussen, T. & Thygesen, K. S. Temperature effects on quantum interference in molecular junctions. *Phys. Rev. B* **89**, 085420 (2014).
180. Hartle, R., Butzin, M., Rubio-Pons, O. & Thoss, M. Quantum interference and decoherence in single-molecule junctions: how vibrations induce electrical current. *Phys. Rev. Lett.* **107**, 046802 (2011).
181. Bergfield, J. P., Solomon, G. C., Stafford, C. A. & Ratner, M. A. Novel quantum interference effects in transport through molecular radicals. *Nano Lett.* **11**, 2759–2764 (2011).
182. Markussen, T., Stadler, R. & Thygesen, K. S. The relation between structure and quantum interference in single molecule junctions. *Nano Lett.* **10**, 4260–4265 (2010).
183. Andrews, D. O., Solomon, G. C., Van Duyne, R. P. & Ratner, M. A. Single molecule electronics: Increasing dynamic range and switching speed using cross-conjugated species. *J. Am. Chem. Soc.* **130**, 17309–17319 (2008).
184. Magoga, M. & Joachim, C. Conductance of molecular wires connected or bonded in parallel. *Phys. Rev. B* **59**, 16011–16021 (1999).
185. Nozaki, D., Avdoshenko, S. M., Sevinçli, H., Gutierrez, R. & Cuniberti, G. Prediction of quantum interference in molecular junctions using a parabolic diagram: understanding the origin of Fano and anti-resonances. *J. Phys. Conf. Ser.* **427**, 012013 (2013).
186. Ke, S. H., Yang, W. & Baranger, H. U. Quantum-interference-controlled molecular electronics. *Nano Lett.* **8**, 3257–3261 (2008).
187. Cardamone, D. M., Stafford, C. A. & Mazumdar, S. Controlling quantum transport through a single molecule. *Nano Lett.* **6**, 2422–2426 (2006).
188. Baer, R. & Neuhauser, D. Phase coherent electronics: a molecular switch based on quantum interference. *J. Am. Chem. Soc.* **124**, 4200–4201 (2002).
189. Garner, M. H. et al. Comprehensive suppression of single-molecule conductance using destructive σ -interference. *Nature* **558**, 415–419 (2018).
190. Baghernejad, M. et al. Electrochemical control of single-molecule conductance by Fermi-level tuning and conjugation switching. *J. Am. Chem. Soc.* **136**, 17922–17925 (2014).
191. Liu, X. et al. Gating of quantum interference in molecular junctions by heteroatom substitution. *Angew. Chem. Int. Ed.* **56**, 173–176 (2017).
192. Venkataraman, L. et al. Electronics and chemistry: varying single-molecule junction conductance using chemical substituents. *Nano Lett.* **7**, 502–506 (2007).
193. Lo, W. Y., Bi, W., Li, L., Jung, I. H. & Yu, L. Edge-on gating effect in molecular wires. *Nano Lett.* **15**, 958–962 (2015).
194. Li, L., Lo, W. -Y., Cai, Z., Zhang, N. & Yu, L. Proton-triggered switch based on a molecular transistor with edge-on gate. *Chem. Sci.* **7**, 3137–3141 (2016).
195. Li, R. et al. Switching of charge transport pathways via delocalization changes in single-molecule metallacycles junctions. *J. Am. Chem. Soc.* **139**, 14344–14347 (2017).
196. Yang, G. et al. Protonation tuning of quantum interference in azulene-type single-molecule junctions. *Chem. Sci.* **8**, 7505–7509 (2017).
197. Ismael, A. K. et al. Side-group-mediated mechanical conductance switching in molecular junctions. *Angew. Chem. Int. Ed.* **56**, 15378–15382 (2017).
198. Gu, C., Jia, C. & Guo, X. Single-molecule electrical detection with real-time label-free capability and ultrasensitivity. *Small Methods* **1**, 1700071 (2017).
199. Sorgenfrei, S. et al. Label-free single-molecule detection of DNA-hybridization kinetics with a carbon nanotube field-effect transistor. *Nat. Nanotechnol.* **6**, 126–132 (2011).
200. Choi, Y. K. et al. Single-molecule lysozyme dynamics monitored by an electronic circuit. *Science* **335**, 319–324 (2012).
201. Bouilly, D. et al. Single-molecule reaction chemistry in patterned nanowells. *Nano Lett.* **16**, 4679–4685 (2016).
202. Xin, N. & Guo, X. Catalyst: the renaissance of molecular electronics. *Chem* **3**, 373–376 (2017).
203. Wen, H. et al. Complex formation dynamics in a single-molecule electronic device. *Sci. Adv.* **2**, e1601113 (2016).
204. Aragonés, A. C. et al. Electrostatic catalysis of a Diels–Alder reaction. *Nature* **531**, 88–91 (2016).
205. Guan, J. et al. Direct single-molecule dynamic detection of chemical reactions. *Sci. Adv.* **4**, eaar2177 (2018).
206. Zhou, C. et al. Direct observation of single-molecule hydrogen-bond dynamics with single-bond resolution. *Nat. Commun.* **9**, 807 (2018).
207. Huang, C. et al. Single-molecule detection of dihydroazulene photo-thermal reaction using break junction technique. *Nat. Commun.* **8**, 15436 (2017).
208. Gu, C. et al. Label-free dynamic detection of single-molecule nucleophilic-substitution reactions. *Nano Lett.* **18**, 4156–4162 (2018).
209. Van Hal, P. A. et al. Upscaling, integration and electrical characterization of molecular junctions. *Nat. Nanotechnol.* **3**, 749–754 (2008).
210. Bergren, A. J. et al. Musical molecules: the molecular junction as an active component in audio distortion circuits. *J. Phys. Condens. Matter* **28**, 094011 (2016).

Acknowledgements

The authors thank M. Schott and Y. Feng for giving feedback on the manuscript. The authors acknowledge primary financial support from the National Key R&D Program of China (2017YFA0204901; X.G.), the National Natural Science Foundation of China (21727806; X.G.), the National Science Foundation of Beijing (Z181100004418003; X.G.), Northwestern University (J.F.S. and M.A.R.), the Israel–US Binational Science Foundation (A.N.), the German Research Foundation (DFG TH 820/11–1; A.N.), the US National Science Foundation (grant no. CHE1665291; A.N.) and the University of Pennsylvania (A.N.).

Author contributions

All authors researched data for the article and contributed to the discussion of content, as well as the writing and editing of the article, before submission.

Competing interests

The authors declare no competing interests.

Publisher's note

Springer Nature remains neutral with regard to jurisdictional claims in published maps and institutional affiliations.